

TABLE OF CONTENTS

LIST OF FIGURES	ixx
LIST OF TABLES	xii
CHAPTER 1. INTRODUCTION	1
CHAPTER 2. BACKGROUND	3
2.1. Definition of Sandwich Structures	3
2.2. Application Areas of Sandwich Structures	6
2.3. Behavior of Sandwich Structures	6
2.4. Constituents of Composite Sandwich Structures	11
2.4.1. Facesheet Materials	11
2.4.1.1. Composite Facesheets	12
2.4.1.1.1. Facesheet Matrix Materials	12
2.4.1.1.2. Facesheet Reinforcement Materials	14
2.4.2. Core Materials	15
2.5. Manufacturing Methods of Sandwich Structures	16
2.5.1. Hand Lay-up	16
2.5.2. Resin Transfer Molding	17
2.5.3. Vacuum Assisted Resin Transfer Molding	17
2.5.4. Vacuum Bagging	18
CHAPTER 3. EXPERIMENTAL	19
3.1. Materials	19
3.2. Fabrication of Composite Sandwich Structures	20
3.3. Characterization Technique	20
3.3.1. Honeycomb Core Material	20
3.3.1.1. Flatwise Mechanical Compression Test	20
3.3.1.2. Optical Microscopy	22
3.3.2. Facesheet Material	22
3.3.2.1. Measurement of Fiber Volume Fraction	22

3.3.2.2. Tensile Test	22
3.3.2.3. Compression Test	23
3.3.2.4. Flexural Test	24
3.3.2.5. Interlaminar Shear Test	25
3.3.3. Composite Sandwich Structure	26
3.3.3.1. Flatwise Compression Test	26
3.3.3.2. Edgewise Compression Test	26
3.3.3.3. Three Point Bending Test	27
3.3.3.4. Mode I Interlaminar Fracture Toughness Test	29
CHAPTER 4. MODELING COMPOSITE SANDWICH STRUCTURES	30
4.1. Modeling Sandwich Structures	30
4.1.1. Micromodeling	32
4.1.2. Macromodeling	33
4.1.3. Classical Lamination Theory	33
4.2. Numerical Modeling of Composite Sandwich Structures	35
4.2.1. Modeling of Facesheets	37
4.2.2. Modeling of Honeycomb Core	38
4.2.3. Modeling of Sandwich Structures	38
CHAPTER 5. RESULTS AND DISCUSSION	41
5.1. Properties of Honeycomb Core	41
5.1.1. Flatwise Compression Properties	41
5.1.2. Cell Wall Thickness	43
5.2. Properties of Facesheet Material	43
5.2.1. Fiber Volume Fraction	43
5.2.2. Tensile Properties	44
5.2.3. Compressive Properties	44
5.2.4. Flexural Properties	46
5.2.5. Interlaminar Shear Properties	47
5.3. Properties of Composite Sandwich Structures	47
5.3.1. Flatwise Compressive Properties	47
5.3.2. Edgewise Compressive Properties	50
5.3.3. Flexural Properties	53

5.3.4. Interlaminar Fracture Toughness	55
5.4. Comparison of Numerical and Experimental Results.....	56
5.4.1. Facesheet Material	56
5.4.2. Honeycomb Core	57
5.4.3. Sandwich Structure	58
CHAPTER 6. CONCLUSION	60
REFERENCES.....	62

LIST OF FIGURES

<u>Figure</u>	<u>Page</u>
Figure 2.1. Main components of sandwich structures.....	4
Figure 2.2. Sandwich structure in comparison with an I- Beam.....	5
Figure 2.3. Different failure modes observed in rotor blades	8
Figure 3.1. Illustration of PP based honeycomb core material	19
Figure 3.2. Flowchart of fabrication process of composite sandwich structure.....	20
Figure 3.3. Flatwise compression test specimen under loading.....	21
Figure 3.4. Tensile test specimen during the test	23
Figure 3.5. Flexural test specimen under loading and test configuration	24
Figure 3.6. SBS test configuration	25
Figure 3.7. Edgewise compression specimen under loading	27
Figure 3.8. Sandwich structure dimensions.....	28
Figure 4.1. An illustration of the physical simulation process.....	32
Figure 4.2. A laminate with different fiber orientations	34
Figure 4.3. Element SHELL181 geometry.....	36
Figure 4.4. Element SHELL 91 geometry.....	37
Figure 4.5. Model of the facesheet tensile test specimen.....	38
Figure 4.6. Honeycomb core cell wall optimization study	39
Figure 4.7. Three point bending test specimen with 5 mm core thickness	40
Figure 5.1. Flatwise compressive behavior of PP based honeycomb core material for each thickness	42
Figure 5.2. Core compressive modulus and strength values with respect to core thickness.....	42
Figure 5.3. Cell wall thickness variation with respect to core thickness	43
Figure 5.4. Typical tensile stress-strain response of E-glass fiber/epoxy composite facesheets.....	44
Figure 5.5. Stress strain behavior of the compressive properties of facesheet material along ply-lay up and in-plane directions	45
Figure 5.6. Failure direction of the ply-lay up specimen loaded in compression test.....	45

Figure 5.7. Typical stress vs. strain curve for the composite facesheets under flexural loading	46
Figure 5.8. Behaviour of composite sandwich structures under flatwise loading: (a) collapse sequence images, (b) load-deformation graph of the test specimen and the specific absorbed energy, $E_{s,a}$ graph during the test.....	48
Figure 5.9. Flatwise compressive strength and modulus values of composite sandwich structures as a function of core thickness	49
Figure 5.10. Failure mechanisms for sandwich structures with various core thicknesses under flatwise compression loading (The stroke is 3 mm for each core).....	49
Figure 5.11. Specific absorbed energy values of the composite sandwich structures with respect to core thickness increment.....	50
Figure 5.12. Behaviour of the composite sandwich structures under edgewise loading: (a) collapse sequence images of the specimen and (b) load-deformation graph of the test specimen and the specific absorbed energy, $E_{s,a}$ during the test	51
Figure 5.13. Facesheet compressive stress as a function of core thickness increment	52
Figure 5.14. Failure mechanisms for sandwich structures with all different core thicknesses under edgewise compression loading.....	52
Figure 5.15. Energy absorption values of the composite sandwich structures with core thickness increment.....	53
Figure 5.16. Core shear stress and sandwich beam deflection tendency with increasing core thickness	54
Figure 5.17. Panel bending stiffness and panel shear rigidity tendency of the composite sandwich structures with core thickness increase under flexural loading	54
Figure 5.18. Facesheet bending stress of the composite sandwich structures with core thickness increment.....	55
Figure 5.19. Interlaminar fracture toughness values of the composite sandwich structures with respect to the core thickness increment.....	56
Figure 5.20. Deformed and undeformed shape of the facesheet tensile test specimen	57

Figure 5.21. Comparison of predicted and experimental data of facesheet tensile test.....	57
Figure 5.22. Force deformation graph of experimental and predicted flatwise compression test data.....	58
Figure 5.23. Predicted and experimental force deformation comparison graph of the sandwich structure	59

LIST OF TABLES

<u>Table</u>	<u>Page</u>
Table 3.1. Specimen dimensions for edgewise compression test.....	27
Table 3.2. Specimen dimensions for three point bending test.....	29

CHAPTER 1

INTRODUCTION

The use of composite sandwich structures in aerospace and civil infrastructure applications has been increasing especially due to their extremely low weight that leads to reduction in the total weight and fuel consumption, high flexural and transverse shear stiffness, and corrosion resistance (ASM Handbook 1987). In addition, these materials are capable of absorbing large amounts of energy under impact loads which results in high structural crashworthiness. In its simplest form a structural sandwich, which is a special form of laminated composites, is composed of two thin stiff facesheets and a thick lightweight core bonded between them. A sandwich structure will offer different mechanical properties with the use of different types of materials because the overall performance of sandwich structures depends on the properties of the constituents (Daniel 2008). Hence, optimum material choice is often obtained according to the design needs (Vinson 1999). Various combinations of core and facesheet materials are utilized by researchers worldwide in order to achieve improved crashworthiness (Adams 2006).

In a sandwich structure generally the bending loads are carried by the force couple formed by the facesheets and the shear loads are carried by the lightweight core material (Nguyen, et al. 2005). The facesheets are strong and stiff both in tension and compression as compared to the low density core material whose primary purpose is to maintain a high moment of inertia. The low density of the core material results in low panel density, therefore under flexural loading sandwich panels have high specific mechanical properties relative to the monocoque structures. Therefore, sandwich panels are highly efficient in carrying bending loads. Under flexural loading, face sheets act together to form a force couple, where one laminate is under compression and the other under tension. On the other hand, the core resists transverse forces and stabilizes the laminates against global buckling and local buckling (Glenn and Hyer 2005). Additionally, they provide increased buckling and crippling resistance to shear panels and compression members (Smith and Shivakumar 2001).

The critical properties of sandwich structures vary according to the application area of the structure. In automotive industry the out of plane compressive properties are more critical, whereas in wind turbines the in plane compressive properties are more important. Therefore, depending on the application area, different properties or characteristics of sandwich panels are needed to be evaluated (Davies, et al. 2004).

In order to select the correct configuration for the sandwich structures according to the design specifications, the most widely used way is numerically model them (Marques 2008). For this purpose, finite element modeling is used worldwide and the behavior of the structures can be seen before manufacturing the real parts.

The objectives of this study is to understand the mechanical behavior and failure mechanisms of sandwich structures with polypropylene (PP) based honeycomb core and glass fiber reinforced polymer (GFRP) facesheets fabricated by hand lay up technique as a function of core thickness. For this purpose, flatwise compression (FC), edgewise compression (EC), Mode I interlaminar fracture toughness and three point bending (3PB) tests were conducted on composite sandwich specimens with various core thicknesses. Constituents of the sandwich structures were also tested mechanically and the results of these tests were used as input for the finite element modeling by using ANSYS software.

CHAPTER 2

BACKGROUND

Composite materials consist of two or more different materials bonded to each other in order to utilize the properties of each constituent for the structural improvement of the whole assembly. Composite materials prevail over traditional monolithic engineering materials as they offer several advantages such as high strength, high stiffness, long fatigue life, low density, wear and corrosion resistance and acoustic insulation. The reason that composites have superior structural performance is their high specific strength (strength to density ratio) and high specific stiffness (modulus to density ratio). Because of this reason composite parts are lighter than their counterparts. Therefore they have wide usage in automotive industry because of fuel efficiency in transportation vehicles, in addition to the marine structures, infrastructures and defense applications. Moreover, they offer design flexibility and alternative manufacturing routes. (Turgut 2007, Ercan 2006).

There are three main classifications of composite materials: particle-reinforced, fiber-reinforced, and structural composites. In particle-reinforced composites, particle dimensions are approximately the same in all directions and generally particulate phase is harder and stiffer than the matrix. In fiber-reinforced composites, the dispersed phase has the geometry of a fiber, the mechanical properties mostly depend on the properties of the fibers and applied load is transmitted to the fibers by the matrix phase through the fiber/matrix interface. Structural composites are the combinations of composites and homogeneous materials and the geometrical design of the structural elements affect the mechanical properties of the structure. The most common structural composites are laminated composites and sandwich panels (Callister 1999).

2.1. Definition of Sandwich Structures

A sandwich structure is a special form of laminated composites. A typical sandwich structure consists of two thin, high strength facesheets bonded to a thick, light weight core (Figure 2.1). Facesheets are rigid and core is relatively weak and flexible,

but when combined in a sandwich panel they produce a structure that is stiff, strong and lightweight (Rocca and Nanni 2005).

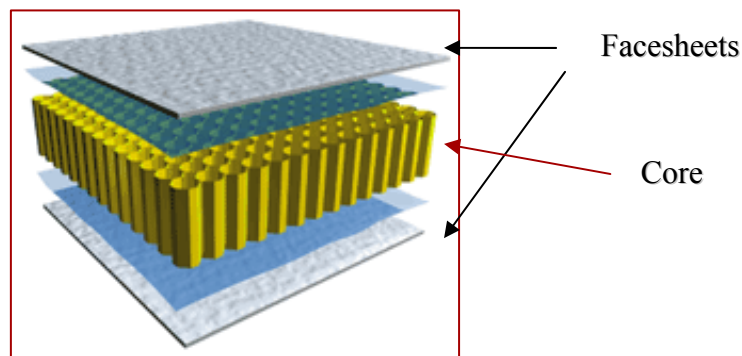


Figure 2.1. Main components of sandwich structures

In structural sandwiches, facesheets are mostly identical in material and thickness and they primarily resist the in-plane and bending loads. These structures are called symmetric sandwich structures. However, in some special cases facesheets may vary in thickness or material because of different loading conditions or working environment. This configuration is named as asymmetric sandwich structures.

In general sandwich structures are symmetric; the variety of sandwich constructions basically depends on the configuration of the core. The core of a sandwich structure can be almost any material or architecture, but in general they are classified in four types; foam or solid core, honeycomb core, web core and corrugated or truss core. The adhesion of facesheets and core is another important criterion for the load transfer and for the functioning of the sandwich structure as a whole (Rocca and Nanni 2005, ASM Handbook 1987).

The basic concept of a sandwich structure is that the facesheets carry the bending loads while the core carries the shear loads. The facesheets are strong and stiff in tension and compression compared to the low density core material whose primary purpose is to keep the facesheets separated in order to maintain a high section modulus (a high “moment of inertia” or “second moment of the area”) (Adams 2006). The core material has relatively low density (e.g., honeycomb or foam), which results in high specific mechanical properties, in particular, high flexural strength and stiffness properties relative to the overall panel density. Therefore, sandwich panels are efficient in carrying bending loads. Additionally they provide increased buckling resistance to shear panels and compression members. Sandwich construction results in lower lateral

deformations, higher buckling resistance and higher natural frequencies than monocoque constructions (Vinson 1999, Adams 2006).

A sandwich structure operates in the same way with the traditional I-beam, which has two flanges and a web connecting the flanges (Figure 2.2). The connecting web makes it possible for the flanges to act together and resist shear stresses. Sandwich structure and an I-beam differ from each other that, in a sandwich structure the core and laminates are different materials and the core provides continuous support for the laminates rather than being concentrated in a narrow web. When the structure subjected to bending the laminates act together, resisting the external bending moment so that one laminate is loaded in compression and the other in tension. The core resists transverse forces, at the same time, supports the laminates and stabilizes them against buckling and wrinkling (local buckling) (Norlin and Reuterlöv 2002).

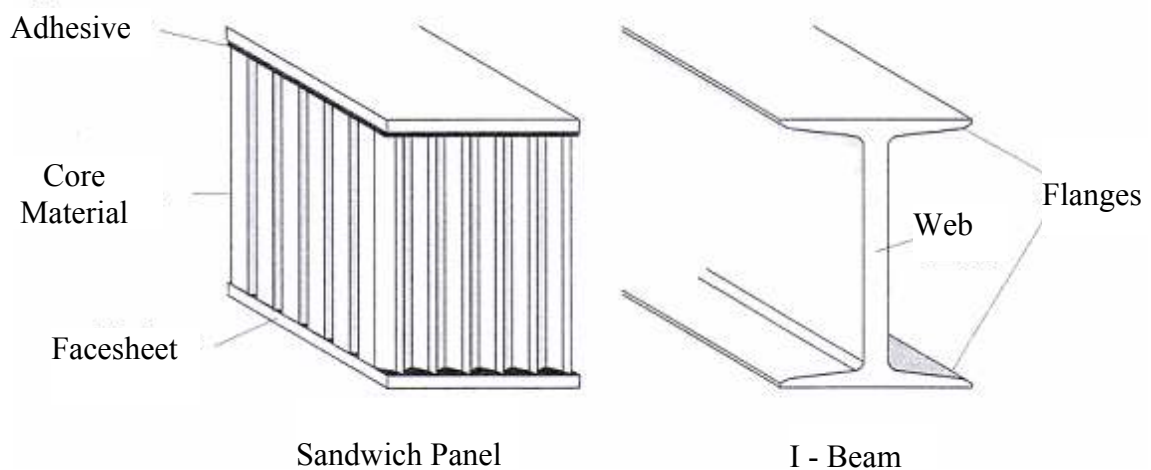


Figure 2.2. Sandwich structure in comparison with an I-Beam
(Source: Göde 2007)

Sandwich structures should be designed to meet the basic structural criteria such as the facesheets should be thick enough to withstand the tensile, compressive and shear stresses and the core should have sufficient strength to withstand the shear stresses induced by the design loads. Adhesive must have sufficient strength to carry shear stress into core. The core should be thick enough and have sufficient shear modulus to prevent overall buckling of the sandwich under load to prevent crimping. Compressive modulus of the core and the facesheets should be sufficient to prevent wrinkling of the facesheets under design load. The core cells should be small enough to prevent the facesheet

dimpling under design load. The core should have sufficient compressive strength to resist crushing design loads acting normal to the panel facesheets or by compressive stresses induced through flexure. The sandwich structure should have sufficient flexural and shear rigidity to prevent excessive deflections under design load (ASM Handbook 1987). In order to sustain these criteria, sandwich structures may also be produced as complex structures that include localized reinforcements in the form of FRP tubes, cones or corrugation connecting the external face plates (Mamalis, et al. 2005).

2.2. Application Areas of Sandwich Structures

The use of composite sandwich structures in aeronautical, automotive, aerospace, marine and civil engineering applications is getting wider as these structures have excellent stiffness to weight ratios that leads to weight reduction and fuel consumption. Also they have high structural crashworthiness because they are capable of absorbing large amounts of energy in a sudden collision. Various combinations of core and facesheet materials are being studied by researchers worldwide in order to achieve improved crashworthiness (Mamalis, et al. 2005).

In aerospace applications various honeycomb cored sandwich structures were used for space shuttle constructions also they are used for both military and commercial aircrafts. The U.S. Navy and the Royal Swedish Navy has used honeycomb sandwich bulkhead to reduce the weight of the ship and to withstand underwater explosions for more than 20 years. Moreover, locomotives are designed in order to resist the pressure waves occurring during the crossing of two high-speed trains in tunnels. More recently, sandwich constructions are commonly used in civil engineering projects such as bridge decks, wall and roof claddings for buildings because of their low cost and thermal performance. Also, railcars for rapid transit trains, busses, sailboats, racing boats, racing cars, snow skis, water skis and canoes are all employing sandwich constructions (Vinson 1999).

2.3. Behavior of Sandwich Structures

The critical properties of the sandwich structures vary according to the application area of the structure. In automotive industry the out of plane compressive properties are more important whereas in the wind turbines, the in plane compressive

properties are more significant. Therefore, different properties or characteristics of the sandwich panel are needed to be evaluated according to the application area (Adams 2006).

Norlin and Reuterlöv (2005) studied the primary loads applied to the wind turbine blades. The sandwich sections in the turbine blades are subjected to a complex combination of in-plane and out-of-plane stresses that need to be taken into account in the design, engineering and fabrication steps of turbine blades. These effects may cause different failure modes as seen in Figure 2.3. Failure modes (a) and (b) are a result of out-of-plane loading where in (a) the laminates fail in either compression or tension, and in (b) the core material fails in shear. Failure modes (c) and (d) are described as local buckling. Failure can occur in two ways, in the first type a wrinkle that becomes unstable may cause an indentation or the laminate may buckle outwards. These defects are caused by inadequate compression modulus values of the core or facesheets. Thus, the resistance towards laminate buckling depends on three properties; the bending modulus of the laminate, the shear modulus and the compression or tension modulus of the core material. Two out of three properties are core material related. Therefore, the most effective way to improve the in-plane properties is to increase the core thickness and core density.

Failure mode (e) is known as general buckling and is caused by in-plane loading. In in-plane loading of the sandwich structures, collapse modes are also important and in order to investigate the compressive properties, collapse modes and crushing characteristics of various types of composite sandwich panels. Mamalis et al. (2005) carried out a series of edgewise compression tests by eight different material combinations made of four types of polymer foam core (PMI foam, two grades of linear PVC foam and polyurethane foam) and two types of FRP facesheet laminates made of glass fiber/acrylic resin. Under edgewise compressive load, sandwich panels tend to collapse in three different modes, two of them were unstable (overall column buckling mode I with foam core shear failure and mode II sandwich disintegration with facesheet delamination and buckling to opposite directions) while the third one was stable progressive end-crushing mode. Unstable crushing with overall column buckling is the most probable mode of collapse while progressive end-crushing is the less expected one. The most important factor that determines the collapse mode and the overall crushing response of a sandwich panel in edgewise compression is the properties and

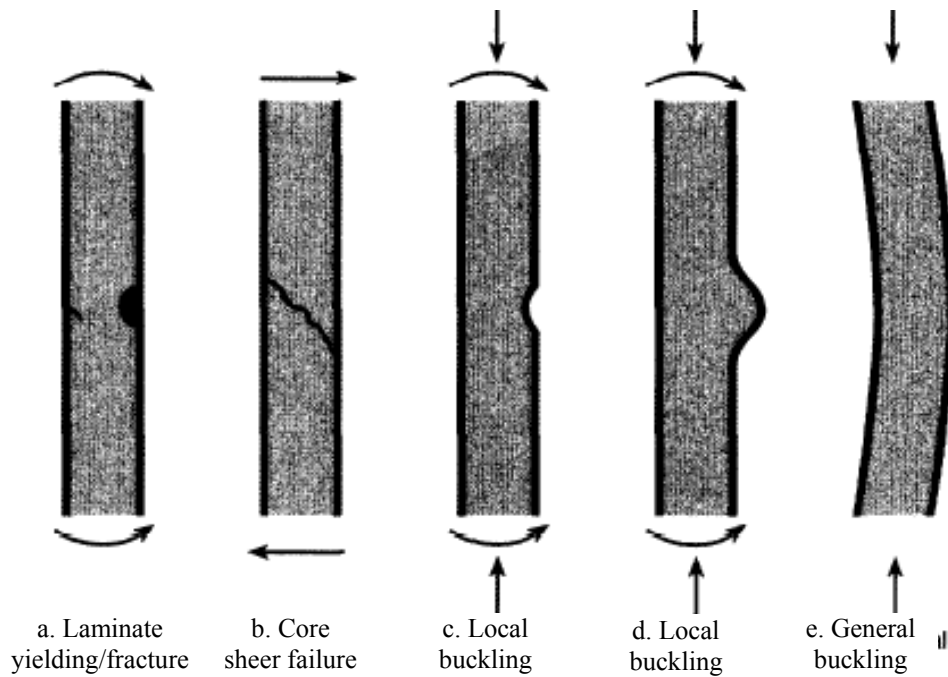


Figure 2.3. Different failure modes observed in rotor blades

(Source: Norlin and Reuterlöv 2005)

strength of the foam core. Column buckling collapse mode was observed in the case of panels produced by the weaker foam core. In the progressive collapse mode, foam core has the highest density, highest modulus of elasticity, highest shear strength and elongation at break compared to all others. Among the three collapse modes the most efficient one with respect to crash energy absorption is the progressive end-crushing mode that the sandwich components contribute to energy dissipation and continued to resist to compressive deformation and progressive crushing as an integral structure while in modes I and II sandwich structure was partially or totally disintegrated.

Smith and Shivakumar (2001) and Cantwell et al. (1999) focused on the fracture toughness of the sandwich structures. Smith and Shivakumar (2001) used Cracked Sandwich Beam (CSB) test configuration to test five different sandwiches manufactured using VARTM with varying core densities of PVC cores. It was observed that fracture toughness values increase with respect to the core density but they are not dependant on the facesheet material. Cantwell et al. (1999) had developed simple test geometry in order to test glass fiber/balsa sandwich structures and pre-cracked sandwich beams are loaded as in the three-point-bending test. At low loading rates the interfacial fracture toughness was found to be quite high but at high loading rates significant reductions were observed for some of the sandwich materials. This result was significant while

these materials are used in marine structures which are subjected to dynamic loads such as wave slamming or blast loading.

The fatigue behavior of the sandwich composites mainly depends on the damage mechanisms such as matrix cracking, fiber bridging in the skins and interfacial debonding between core and skin, and shear cracks in the core. El Mahi et al. (2004) studied the fatigue behavior in three point bending loading. The sandwich composites were made of PVC foams, different composite facesheets and constructed by hand lay-up/vacuum bagging technique. It was observed that evolution of damage in displacement and load controls are quite different in fatigue. In displacement control, growth of damage is very fast in initial number of cycles. In load control, the specimen received damages due to fatigue with the increase in number of cycles. Therefore, the type of loading plays an important role as it controls the type of damage in sandwich composites.

Rocca and Nanni (2005) studied static compressive and fatigue compressive behaviors of sandwich panels manufactured with a new type of core made of closed cell foam combined with dry fibers and GFRP facings. In static compressive tests, buckling of the facesheet and the creation of gaps in between the foam and the facesheets was observed. The facesheets buckled originating vertical cracks or gaps and bending of the foam in the transverse direction. In fatigue compressive test, no considerable reduction in the compressive capacity of the material was observed.

Buckling behavior of the sandwich structures is also important and Davalos and Chen (2005) studied this case under out-of-plane compressive loading. Bare compression and stabilized compression tests (specimen was bonded between steel plates in this test) were performed and it was observed that failure loads were higher than those for the bare compression tests but buckling occurred only for the bare compression tests as the stabilized compression test induced material compression failure.

Davies et al. (2004) produced two types of sandwich panels with carbon epoxy skins and aluminum honeycomb core. These panels were subjected to low velocity impacts and then the damaged panels tested for their compression-after-impact (CAI) strength. Thick-facesheet, thin-core option of the panels was found to be good energy absorber. The thin-facesheet, thick-core panels were damaged easily. In the tests, debonding did not occur between upper facesheet and core but massive debonding took place between the lower facesheet and the core when the impactor penetrated the

facesheet. The thick-skin, thin-core panel absorbed most of the impact and after the impact its compressive strength was reduced.

Modelling results on the mechanical behavior of the sandwich structures have been also reported in the literature. Borsellino et al. (2004) used commercial ANSYS code in order to model the sandwich structures in compressive, shear and flexural loadings. The static-mechanical behavior of the composite structure was well approximated by numerical simulations in the elastic zone but in the plastic regime there was not a compatibility with the experimental data.

Liang and Chen (2006) performed a theoretical work to obtain an accurate solution for the difficulty caused by the structural complexity of honeycomb sandwich panel. They investigated the perpendicular stress components in honeycomb sandwich panels and the 3D finite element numerical simulation was built up that validates the critical compressive stress diagram. To obtain a rational thickness of the honeycomb sandwich panel, the new iterative optimization design method was presented.

Smith and Shivakumar (2001) performed finite-element analyses (FEA) for the CSB test configuration. The test results indicated that the fracture toughness is independent of crack length and constant. Two-dimensional finite-element models of the modified Mode-I CSB test was able to reproduce the critical load values obtained from the fracture tests.

Jianga et al. (2004) studied the existing two fracture mechanisms in facesheets of sandwich composites consisting of the 0° and 90° plies, namely crack growth and crack blocking. The former was undesired since it may lead to the failure of facesheets in sandwich composites. A shear-lag model that gives a simple criterion governing these two mechanisms was developed. It was established that, for a given ratio of $E_t = E_f$ (the elastic modulus in the transverse and fiber directions respectively), there exists a critical facesheet thickness above which crack blocking is achieved and crack growth is prevented. Equivalently, for a given facesheet thickness b ; there exists a critical elastic modulus ratio E_r/E_f below which the crack blocking is ensured. For $b = 6t$ (t is the ply thickness), E_f was found to be more than 23 times larger than the E_t in order to ensure the crack blocking. For $b \geq 20t$; E_f was found to be only 10 times larger than E_r .

2.4. Constituents of Composite Sandwich Structures

There are various types of facesheet and core materials and every different combination of these components results with sandwich constructions having different mechanical behaviors. It is important to produce a sandwich structure having required properties according to the working environment. In order to employ the proper components the following conditions must be satisfied:

1. determination of the absolute minimum weight for a given structural geometry, loading and material system
2. comparison of one type of sandwich construction with others
3. comparison of the best sandwich construction with alternative structural configurations (monocoque, rib-reinforced, etc.)
4. selection of the best facesheet and core materials in order to minimize structural weight
5. selection of the best stacking sequence for faces composed of laminated composite materials
6. comparison of the optimum construction weight with weights required by some restrictions; i.e., the weight penalty due to restrictions of cost, minimum gage, manufacturing, material availability, etc.

Main components of the composite sandwich structures are investigated separately in a detailed manner.

2.4.1.Facesheet Materials

In a sandwich structure the facesheets can be made of many different materials, it can be isotropic monocoque material, anisotropic monocoque material or a composite material. Aluminum, fiberglass, graphite and aramid are the widely used facesheet materials. However, in order to minimize the weight of the structure generally composite facesheets are preferred.

2.4.1.1. Composite Facesheets

The facesheet thickness ranges from 0,25mm to 40 mm according to the design specification. Design flexibility is an advantage for the manufacturer because not only unnecessary material can be removed from areas with little stress also unnecessary weight can be decreased. Another reason to use composite material is that they have superior resistance to most environments and they can be used by most individuals without a major investment in equipment also they can be easily shaped into complex shapes. The aim of the use of the composite material must be clear in order to select proper constituent matrix material and reinforcement.

In these composites, the function of the fiber is carrying the load exerted on the composite structure, and providing stiffness, strength, thermal stability and other structural properties. Matrix material carries out several functions in a composite structure, some which are binding the fibers together and transferring the load to the fibers, and providing protection to reinforcing fibers against chemical attack, mechanical damage and other environmental effects like moisture, humidity, etc (Turgut 2007).

2.4.1.1.1. Facesheet Matrix Materials

The mechanical performance and durability of polymer-matrix based composite laminates is strongly linked to the mechanical performance of the matrix. Since polymers behave as viscoelastic/viscoplastic solids depending on strain/stress rate, even at room temperature. Creep and stress relaxation are other consequences which have to be taken into account during the design. The combined effects of creep, fatigue, moisture and temperature on the mechanical properties and the time to failure are very complex and still under research. The viscoelastic properties of materials can be expected to depend on temperature as well as time. The moisture acts on the polymeric matrix as plasticizer, lowering the glass transition temperature. Also moisture changes the time-dependent mechanical response of the PMCs and the reverse is true, i.e. viscoelastic relaxation process changes the diffusion rate and moisture saturation levels (Guedes 2008).

Selection of the matrix material is an important step and the properties of the matrix materials and manufacturing type of the composite material must be considered carefully. There are two main types of resins, they are thermosetting and thermoplastic resins.

Epoxy, unsaturated polyester and vinyl ester are the most widely used thermosetting resins. Wide range of physical and mechanical properties can be obtained by employing these resins. The formation of rigid solid from liquid resin is done during the composite is being manufactured. The mechanical properties of the resin depend on both the resin chemical and curing chemical. The resin chemical controls the mechanical properties while the curing chemical controls the density and the length of formed network. Curing is generally completed by a schedule involving heating and keeping the resin to one or more levels of temperature at prescribed times. This way the optimum cross-linking and optimum resin properties can be achieved.

When compared to thermoplastics, it can be easily seen that thermoplastics can undergo plastic deformation while thermosets are brittle. However, thermosets have different properties when compared to each other. For example, epoxies are generally tougher than unsaturated polyesters or vinyl esters. Also epoxies have good resistance to heat distortion and they shrink less during curing comparing to the polyester. In fact, epoxy resins are better in most properties than other thermosetting resins. Epoxy is used in weight critical, high strength, and dimensionally accurate applications. Polyester resins are less expensive, offer more corrosion resistance, and are more forgiving than epoxies. For this reason, they are the most widely used. Certain resins are not compatible with all fabrics. For instance, Kevlar often exhibits adhesion problems, so epoxy or the highest grade polyester should be used. Also, fiberglass mats have a polyester soluble binder. Epoxies cannot dissolve this, and should never be used with mat.

Thermoplastic resins are not cross-linked but they are monomer units and have very high molecular weight ensuring there is a high concentration of molecular entanglements acting like cross-links. Thermoplastics, compared to thermosets, have high failure strains, good resistance to chemicals and thermal stability. Many thermoplastics, except nylons, show good resistance to absorption of water.

2.4.1.1.2. Facesheet Reinforcement Materials

The physical properties of composites are fiber dominant. When resin and fiber are combined, their performance remains most like the individual fiber properties. For this reason, fabric selection is critical when designing composite structures. There are many reinforcement materials available to use in matrix systems but all reinforcement materials have high stiffness and relatively low density and they have numerous types and styles. Glass, carbon and aramid fibers are widely used in polymer matrix composites.

Glass fibers are based on silica (SiO_2) with additions of calcium, boron, sodium, iron or aluminum oxides. E-glass (E meaning electrical) is the most commonly used glass fiber since it has good strength, stiffness, electrical and weathering properties. C-glass (C meaning corrosion) is employed where more resistance to corrosion with respect to E-glass is needed, but C-glass has lower strength. For applications where higher strength than E-glass is needed, S-glass (S meaning strength) is used as reinforcement material. S-glass have higher Young's modulus and temperature resistance compared to E-glass.

Glass fibers are produced by the mechanical drawing of the flow of the melted raw materials by the gravity. The control of the diameter of the glass is possible by controlling different parameters like the head level of the melted glass in the tank, the viscosity of the glass and the diameter of the holes that the raw material is drawn. The diameter of the E-glass is generally in between 8-15 μm .

Carbon fiber is a modern reinforcement characterized by extremely low weight, high tensile strength, and high stiffness. The material handles easily and can be molded like fiberglass. However, some advanced techniques are necessary to achieve the maximum properties of this material. Carbon fiber is also the most expensive of the reinforcing fibers. This fact often limits its use. Carbon fibers consist of small crystallites of graphite and generally about 8 μm in diameter.

Aramid fibers are developed from aromatic polyamides and they form the most important high modulus polymer fiber group. Aramid fibers were first developed by Du Pont under the trade name Kevlar™. Kevlar exhibits the lowest density of any fiber reinforcement, high tensile strength for its weight, and superior toughness. It is priced between fiberglass and carbon fiber. Kevlar is puncture and abrasion resistant, making it

the reinforcement of choice for canoes, kayaks, and leading edges of airfoils. On the other hand, Kevlar is difficult to cut and machine during part fabrication. It also has a low service temperature and poor compressive properties. It is possible to combine Kevlar with other materials creating a hybrid laminate to compensate for the shortcomings.

2.4.2. Core Materials

The other main component of the composite sandwich structures is the core material. For all sandwich structures both in-plane and bending (primary loading) are carried by the facesheets, and the core carries transverse shear loads. Usually the facesheets are identical in material and thickness. The variety of types of sandwich constructions basically depends upon the configuration of the core (Rocca and Nanni 2005). To maintain the effectiveness of the sandwich structure the core must be strong enough to withstand the compressive or crushing load placed on the panel. The core also must resist the shear forces involved. If the core collapses, the mechanical stiffness advantage is lost. Core densities range from 16kg/m^3 to 900kg/m^3 (ASM Handbook 1987). The core materials are generally divided into four types. These are foam or solid core, honeycomb core, web core and corrugated or truss core.

Foam or solid cores are relatively expensive and can consist of balsa wood, and an almost infinite selection of foam/plastic materials with a wide variety of densities and shear moduli. Honeycomb-core architectures have been widely used. The two most common types are the hexagonally-shaped cell structure and the square cell. Web core construction is also used analogous to a group of I-beams with their flanges welded together. In the web core and truss core constructions, the space in the core could be used for liquid storage or as a heat exchanger.

There are various types of the foam cores, one of them is the vinyl sheet foam is one of the most versatile core materials on the market. It is a rigid, closed cell material that resists hydrocarbons, sea water, gasoline and diesel oil. It has been used extensively in aircraft and performance automotive structures, but it can be applied anywhere that high properties and easy handling are needed. Vinyl foam can be thermoformed in an oven or with a heat gun while applying gentle pressure. Another foam type is the polyurethane foam which is a rigid, closed cell material with excellent thermal

insulation and flotation properties. This core is widely used in the marine industry for decades and is fairly inexpensive when a lower property cored laminate is needed. It is compatible with both polyester and epoxy resin systems.

Honeycomb is a series of cells, nested together to form panels similar in appearance to the cross-sectional slice of a beehive. In its expanded form, honeycomb is 90-99 percent open space. Honeycomb is fire retardant, flexible, lightweight, and has good impact resistance. It offers the best strength to weight ratio of the core materials. Honeycomb is used primarily for structural applications in the aerospace industry. Honeycomb structures are manufactured by using a variety of different materials, depending on the intended application and required characteristics, from paper or card, used for low strength and stiffness for low load applications, to high strength and stiffness for high performance applications. The strength of laminated or sandwich panels depends on the size of the panel, facing material used and the number or density of the cells within it (Vinson 1999).

It is assumed that in sandwich structures having foam or honeycomb core all of the primary loading is carried by the facesheets. However, in web or truss cored structures a portion of the primary load is carried by the core.

There may be many other core architectures in addition to the mentioned ones above. For example, recent studies propose sandwich structures having composite vertical laminate-reinforced foam.

2.5. Manufacturing Methods of Sandwich Structures

There are different manufacturing methods used in the production of structural composites. These methods include hand lay-up, Vacuum-Assisted Resin Transfer Molding (VARTM), pultrusion, vacuum bag molding, press molding and autoclave molding (Zureick, et al. 1995).

2.5.1. Hand Lay-up

This is a manual approach in which layers of fabric and resin are successively applied onto a mould. This method is perhaps the simplest, oldest and least complicated. The mold is firstly designed to the shape of the final composite structure. The fiber

layers are oriented in such a way as to develop the desired strength and stiffness. After each layer of fabric is placed, a roller is used on the composite so that a strong bond results and excess resin is squeezed out. The stacking of fabric materials and resin is done until the required thickness is achieved. This method is labor intensive and only suitable for production in low volume. It also has a disadvantage of low quality control and inconsistency in properties of various parts of the finished product. However, with this method, complicated shaped composites can be manufactured, such as the complex core configuration of the sinusoidal honeycomb panel. In recent years, the advances in manufacturing technology have resulted in some improvement in this manual process. Today, the hand lay-up has become automated in several applications.

2.5.2. Resin Transfer Molding

In the resin transfer molding (RTM) resin is injected into a mould in which the fibers and the core material are placed in the desired position. The resin is fed under the gravity or external pressure. Curing occurs within the mould, often assisted by heating. The mould is usually made of metal which gives good heat transfer and lasts for many molding operations. Relatively large parts can be manufactured in this way.

2.5.3. Vacuum Assisted Resin Transfer Molding

In this process, dry fabrics needed to produce the structural component are stacked together successively. The fabric is placed in an open mold surface without a top. When the layup operation is completed, the mold is covered, and a vacuum is applied to consolidate the material. Resin is then allowed to flow and disperse through the entire structural network, with the mold kept under vacuum. The resin is cured under ambient conditions. This process has a great advantage of comparatively low cost of production, since the materials, molds, equipments are inexpensive. It is also advantageous over many other methods because of minimized environmental hazards from toxins associated with the process. The mold is sealed during the resin application, thus controlling environmental threats and reducing health risks of workers.

2.5.4. Vacuum Bagging

In this technique, fabrics are wetted by the resin in a mold, the core material is put between the fabrics after the lamination a vacuum bag is sealed on the laminate. By adding pressure to the laminate, excess resin can be eliminated which will reduce overall weight and optimize strength. Vacuum bagging is used in order to add pressure without crushing the part and vacuum is run into the sealed area. The resulting vacuum pressure squeezes out excess resin. A vacuum pump is required and the process is usually conducted while the part is in a mold.

CHAPTER 3

EXPERIMENTAL

3.1. Materials

E-glass non-crimp fabrics, epoxy thermosetting resin and polypropylene based honeycomb core materials were used to fabricate composite sandwich panels. As the reinforcement constituent of the composite facesheets, E-glass 0°/90° biaxial non-crimp fabrics were provided by Telateks Inc., İstanbul. Resoltech™ 1040 epoxy resin with Resoltech™ 1048 amine hardener was used as the matrix material. PP based core material was that has hexagonal cell configuration with an average cell size of 5.5 mm (Figure 3.1) provided by Tubus Waben GmbH & Co.KG. Five different core thicknesses (5, 10, 15, 20 and 40 mm) were used in the fabrication of the composite sandwich panels.

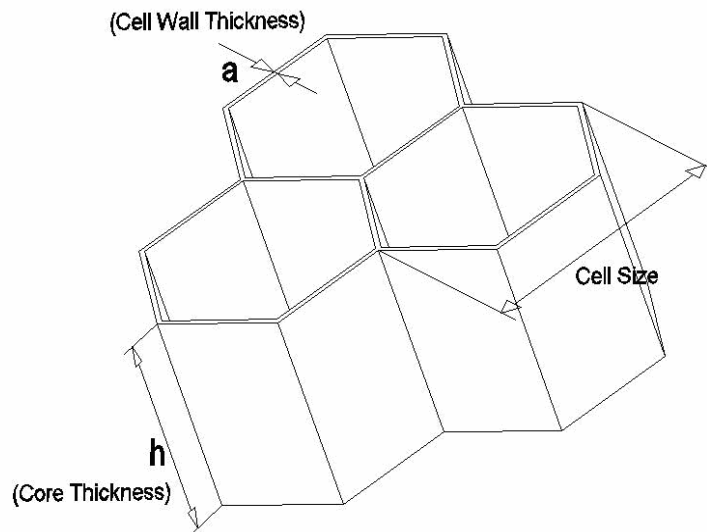


Figure 3.1. Illustration of PP based honeycomb core material

3.2. Fabrication of Composite Sandwich Structures

The sandwich structures were impregnated and laminated by hand lay-up technique. In this technique, six layers of non-crimp glass fabrics were cut in 25 x 25 cm² dimensions. Three layers of fabric were wetted by epoxy resin in order to form lower facesheet and then core material was placed on the lower facesheet, the upper facesheet was laminated with three layers of fabric on the core. Manufacturing process was made in a mold, coated with a mold release agent. After the lamination procedure was completed, composites were cured at room temperature under the pressure of 5 kPa. A post curing for 2 hours at 100°C was applied in an oven after curing. Figure 3.2 shows flow chart of composite sandwich fabrication.

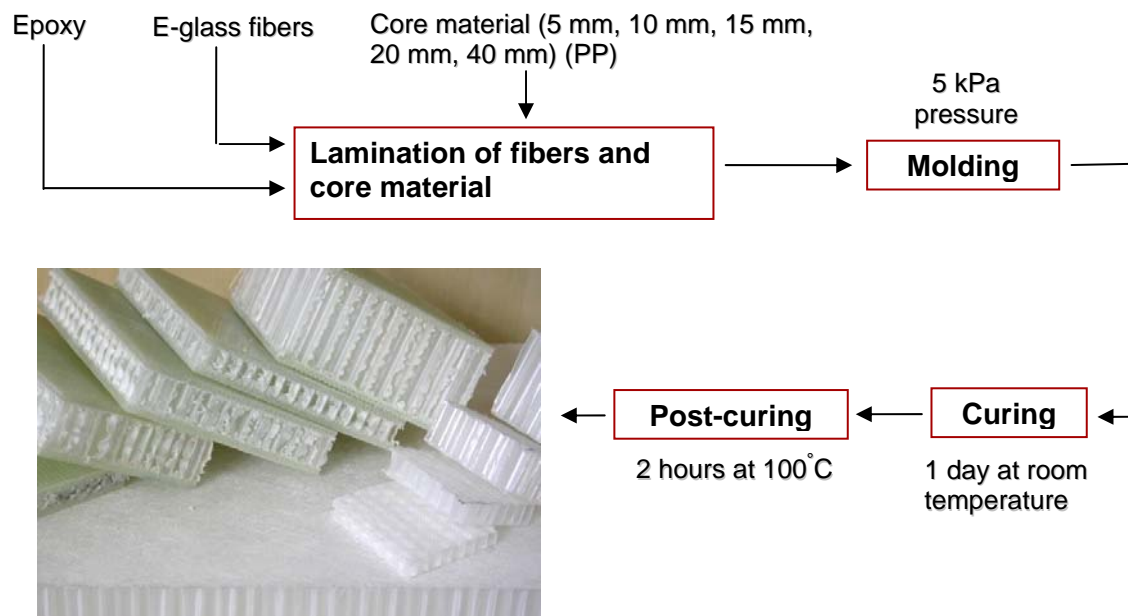


Figure 3.2. Flowchart of fabrication process of composite sandwich structure

3.3. Characterization Technique

3.3.1. Honeycomb Core Material

3.3.1.1. Flatwise Mechanical Compression Test

Flatwise compression test method was used according to ASTM C365-00 in order to determine the compressive strength and modulus of the PP based honeycomb

core material. For this purpose, flatwise compression test specimens were cut into square shape with 52 mm edge dimension for each core thickness from large panels using diamond saw and tests were performed using the mechanical test machine at a crosshead speed of 0.5 mm/min. At least five specimens for each thickness were tested and force versus stroke values were recorded using a Shimadzu™ universal test machine. Figure 3.3 shows a flatwise compression test specimen under loading.

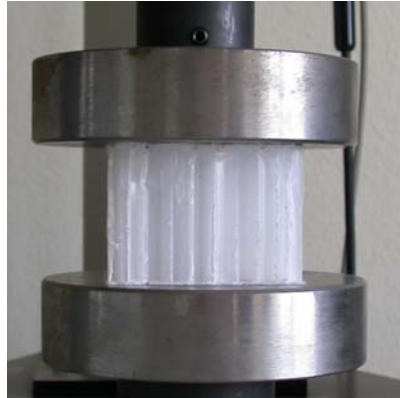


Figure 3.3. Flatwise compression test specimen under loading

The flatwise compressive strength (σ) values were calculated using the following equation;

$$\sigma = \frac{P}{A} \quad (3.1)$$

where P is the ultimate load and A is the cross-sectional area of the specimen. Core compressive modulus (E) values were calculated from the following equation;

$$E = \frac{Sc}{A} \quad (3.2)$$

where S is the slope of the initial linear portion of load-deflection curve ($\Delta P/\Delta u$) and c is the core thickness.

3.3.1.2. Optical Microscopy

Optical microscope was used in order to measure the cell wall thickness of the PP based honeycomb core material. For that reason, Nikon™ optical microscope was utilized. PP based honeycomb core materials with each thickness were cross-sectioned through their mid-thickness planes using utility knife. The cross-sections of the core materials were prepared by metallographic technique.

3.3.2. Facesheet Material

3.3.2.1. Measurement of Fiber Volume Fraction

The burn-out test method was used to determine the fiber volume fraction of the E glass fiber / epoxy facesheets. In this method, sample of about 0.1-0.5 g. of facesheet was burned off in a high temperature oven at about 750°C for about an hour. Then, the remaining fiber mass was weighed and the volume of the fiber was calculated by dividing the mass of the fiber by the density of the fiber material. The fiber volume fraction (V_f) has been calculated as below;

$$V_f = \frac{v_f}{v_f + v_m} \times 100 = \frac{\frac{m_f}{\rho_f}}{\left(\frac{m_f}{\rho_f} + \frac{m_m}{\rho_m}\right)} \times 100 \quad (3.3)$$

where v_f and v_m are the volume of fiber and matrix, m_f and m_m are the mass of fiber and matrix and ρ_f and ρ_m are the density of fiber and matrix, respectively.

3.3.2.2. Tensile Test

Tensile test technique, ASTM D 3039M-93 was used to determine the tensile strength and modulus of the composite facesheets. Test specimens were sectioned from the composite panels with the width of 25 mm, thickness of 3 mm and length of 220 mm. At least five specimens were prepared using a diamond saw. As the facesheet

exhibits similar behaviour for 0° and 90° directions, only one direction is tested. The specimens were tested using Shimadzu™ universal test machine at a cross head speed of 2 mm/min (Figure 3.4).



Figure 3.4. Tensile test specimen during the test

The tensile strength (σ) values were calculated by the following equation;

$$\sigma = \frac{F}{A} \quad (3.4)$$

where F is the ultimate load, and A is the cross sectional area of the specimen. Elastic modulus was obtained from the initial slope of stress (σ) - strain (ε) curves based on the equation below;

$$E = \frac{\sigma}{\varepsilon} \quad (3.5)$$

3.3.2.3. Compression Test

Compression test method according to ASTM D 695-M was used to measure the ply-lay up and in-plane compressive strength and modulus values of the composite facesheet panels. For this purpose, compression test specimens were cut from larger facesheet panels and tests along the in-plane and ply-lay up directions were performed using the mechanical test machine at a crosshead speed of 1.3 mm/min. At least five specimens were tested for each direction and force versus stroke values were recorded

using a Shimadzu™ universal test machine. The compressive stress was calculated by dividing load with cross-sectional area of the specimens. The strain was obtained by dividing stroke with the initial specimen thickness. The modulus was estimated from the slope of the stress - strain curve.

3.3.2.4. Flexural Test

The flexural test method according to ASTM D 790M-03 was used to determine the flexural strength and modulus of the composites. For this purpose, test specimens with 25 mm in width, 3 mm in height and 60 mm in length were sectioned from the facesheet panels using a diamond saw. Specimens were tested in 3-point bending apparatus with a span to thickness ratio of 8. Figure 3.5 shows the flexural test specimen under loading. At least five specimens from composite facesheets were tested using the Shimadzu™ universal test machine at a crosshead speed of 1.2 mm/min. During the test, force vs. deflection of the beam was recorded.

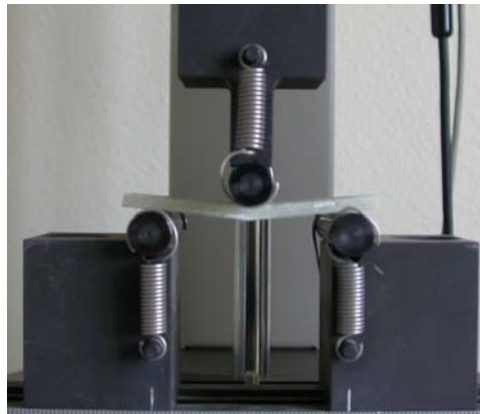


Figure 3.5. Flexural test specimen under loading and test configuration

The flexural strength, S , values were calculated from the equation below;

$$S = \frac{3PL}{2bd^2} \quad (3.6)$$

where P is the applied load at the deflection point, L is the span length; d and b are thickness and width of the specimen, respectively. The maximum strain in the outer fibers occurs at midspan and calculated with the equation below;

$$r = \frac{6Dd}{L^2} \quad (3.7)$$

where r is the maximum strain in the outer fibers, D is the deflection. The flexural modulus values, E_b were calculated with the equation;

$$E_b = \frac{L^3 m}{4bd^3} \quad (3.8)$$

where m is the slope of the tangent to the initial straight line portion of the load-deflection curve.

3.3.2.5. Interlaminar Shear Test

The interlaminar shear strength of the composite specimens was determined performing short beam shear (SBS) tests according to ASTM D2344-00. The SBS specimens 18 mm in length, 3 mm in height and 6 mm in width were cut from the composite facesheets. The length to thickness ratio and span to thickness ratio was 6 and 4, respectively. The crosshead speed was 1 mm/min, five specimens were tested using the Schimadzu™ universal test machine and load at break was recorded. Figure 3.6 shows the SBS test specimen under load.



Figure 3.6. SBS test configuration

The shear strength (τ_{max}) was calculated based on the equation;

$$\tau_{max} = \frac{0.75P_B}{bd} \quad (3.9)$$

where P_B is the breaking load, b and d are the width of the specimen and thickness of the specimen, respectively.

3.3.3. Composite Sandwich Structure

3.3.3.1. Flatwise Compression Test

Flatwise compression test method according to ASTM C 365-00 was used to determine the compressive strength, modulus and to obtain energy absorption characteristics of the composite sandwich panels. For this purpose, compression test specimens were sectioned from larger composite sandwich panels and tests were performed using the mechanical test machine at a crosshead speed of 0.5 mm/min. Test specimens were square shaped with 52 mm edge dimension and at least five specimens were tested and force versus stroke values was recorded using a Schimadzu™ universal test machine. The compressive strength and modulus values were obtained by equation 3.1 and 3.3 similarly with the core material.

3.3.3.2. Edgewise Compression Test

Edgewise compression test method according to ASTM C 364-99 was used to determine the compressive properties of flat structural sandwich construction in a direction parallel to the sandwich facesheet and to obtain energy absorption characteristics and collapse modes of the composite sandwich panels. For this purpose, edgewise compression test specimens were cut with the dimensions given in Table 3.1 from larger composite sandwich panels and tests were performed using the mechanical test machine at a crosshead speed of 0.5 mm/min. At least five specimens were tested and force versus stroke values was recorded using a Schimadzu™ universal test machine. Test configuration and the specimen under edgewise compression loading can be seen in Figure 3.7.

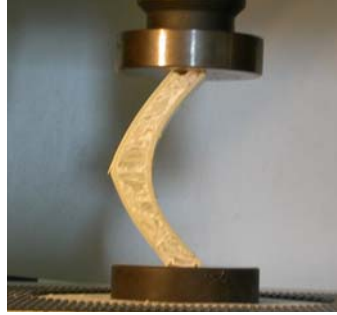


Figure 3.7. Edgewise compression specimen under loading

The facesheet compressive stress (σ) values were obtained by the equation below;

$$\sigma = \frac{P}{A} \quad (3.10)$$

where P is the ultimate load and A is the area of both facings. Specific absorbed energy is obtained by dividing the area under the load-deformation curve by the weight.

Table 3.1. Specimen dimensions for edgewise compression test

Core Thickness	5 mm	10 mm	15 mm	20 mm	40 mm
Specimen dimensions (mm²)	50 × 80	50 × 100	50 × 150	50 × 150	90 × 250

3.3.3.3. Three Point Bending Test

Three point bending test method according to ASTM C 393-00 was used to measure the core shear stress, facing bending stress and panel bending stiffness of the composite sandwich panels. For this purpose, three point bending test specimens were sectioned with the dimensions in Table 3.2 from larger composite sandwich panels and tests were performed using the mechanical test machine at a crosshead speed of 3 mm/min. At least five specimens were tested and force versus stroke values was recorded using Shimadzu™ universal test machine. Core shear stress (τ) values were determined by the equation below;

$$\tau = \frac{P}{(d+c)b} \quad (3.11)$$

where P is load, d is sandwich thickness, c is the core thickness and b is the sandwich width. Facesheet bending stress (σ) is obtained by the equation;

$$\sigma = \frac{PL}{2t(d+c)b} \quad (3.12)$$

where t is facesheet thickness and L is the span length. The dimensions mentioned above can be seen in Figure 3.8.

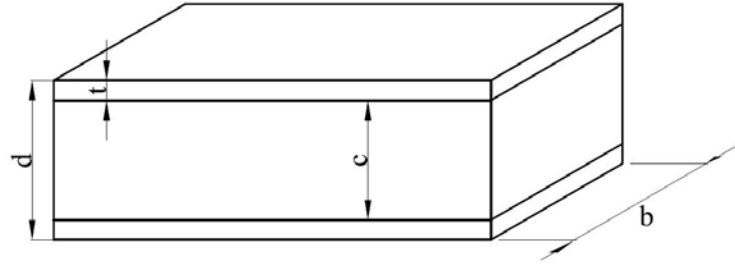


Figure 3.8. Sandwich structure dimensions

Panel bending stiffness (D) is obtained by the formula given below;

$$D = \frac{E(d^3 - c^3)b}{12} \quad (3.13)$$

$$D = \frac{E_1 t_1 E_2 t_2 (d+c)^2 b}{4(E_1 t_1 + E_2 t_2)} \quad (3.14)$$

where E is the facesheet modulus. Equation 3.13 is used for the same facings and equation 3.14 is valid for different facings. In this study facesheets are identical and equation 3.13 is used. Sandwich beam deflection is also calculated in this test method by equation 3.15.

$$\Delta = \frac{PL^3}{48D} + \frac{PL}{4U} \quad (3.15)$$

where Δ is the total beam midspan deflection. In this formula U is the panel bending rigidity and it is calculated by the equation below;

$$U = \frac{G(d+c)^2 b}{4c} \quad (3.16)$$

where G is the core shear modulus.

Table 3.2. Specimen dimensions for three point bending test

Core Thickness	5 mm	10 mm	15 mm	20 mm	40 mm
Specimen Dimensions (mm ²)	25 × 130	32 × 130	42 × 130	52 × 130	92 × 130

3.3.3.4. Mode I Interlaminar Fracture Toughness Test

Mode I interlaminar fracture toughness of the composite sandwich structures was measured using ASTM D 5528-94a test method. The specimens were sectioned from large composite sandwich panels with the width of 20 mm and length of 125 mm for each core thickness. The initial delamination length, a_0 , was about 62.5 mm. The specimens were tested at crosshead speed of 5 mm/min. The cross-head displacement was measured by the universal test machine. Mode I interlaminar fracture toughness, G_{Ic} , values were calculated using the equation below which is based on compliance calibration (CC) method,

$$G_{Ic} = \frac{nP\delta}{2ba} \quad (3.17)$$

where n is the slope of plot of $\text{Log } C$ versus $\text{Log } a$, P is the applied load, δ is the load point deflection, b is the width of DCB specimen and a is the delamination length. For these calculations C is also needed which is the compliance of DCB specimen and is calculated by dividing load point deflection (δ) by the applied load (P).

CHAPTER 4

MODELING COMPOSITE SANDWICH STRUCTURES

4.1. Modeling Sandwich Structures

Mechanics can be divided into three major areas:

- a) Theoretical
- b) Applied
- c) Computational

Theoretical mechanics is concerning about fundamental laws and principles of mechanics. Applied mechanics uses this theoretical knowledge in order to construct mathematical models of physical phenomena and to constitute scientific and engineering applications. Lastly, computational mechanics solves specific problems by simulation through numerical methods on computers.

According to the physical scale of the problem, computational mechanics can be divided into several branches:

- a) Nanomechanics and micromechanics
- b) Continuum mechanics
- c) Systems

Nanomechanics deals with phenomena at the molecular and atomic levels of matter and micromechanics concerns about crystallographic and granular levels of matter and widely used for technological applications in design and fabrication of materials and microdevices. Continuum mechanics is used to homogenize the microstructure in solid and fluid mechanics mainly in order to analyze and design structures. Finally systems are the most general concepts and they deal with mechanical objects that perform a noticeable function.

Continuum mechanics problems can be divided into two other categories:

- a) Statics
 - i. Linear
 - ii. Nonlinear
- b) Dynamics
 - i. Linear
 - ii. Nonlinear

In dynamic cases the time dependency is considered because there is a dependency for the calculations of inertial forces and their derivatives with respect to time. In statics there is no obligation for time dependency and it can also be linear or nonlinear according to the case of interest. Linear static analysis deals with static problems in which the response is linear in the cause and effect sense. Problems outside this domain are classified as nonlinear.

Another classification of the static analysis of continuum mechanics is based on the spatial discretization method by which a problem can be converted to a discrete model of finite number of degrees of freedom:

- a) Finite Element Method (FEM)
- b) Boundary Element Method (BEM)
- c) Finite Difference Method (FDM)
- d) Finite Volume Method (FVM)
- e) Spectral Method
- f) Mesh-Free Method

For linear problems, finite element methods and boundary element methods are widely used. For nonlinear problems finite element methods is unchallengeable (Felippa 2004). In Figure 4.1 the steps in the finite element modeling can be seen.

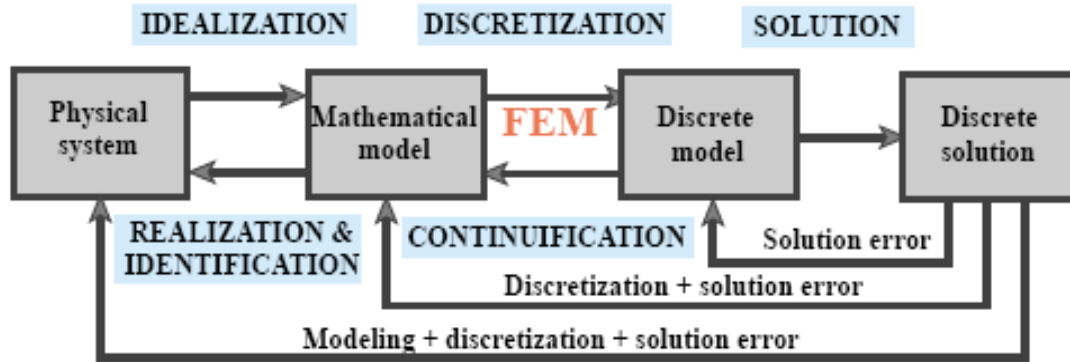


Figure 4.1. An illustration of the physical simulation process

(Source: Felippa 2004)

As it is the issue of this study, the modeling of composite materials is more complex than that of traditional engineering materials. The properties of composites, such as strength and stiffness, are dependent on the volume fraction of the fibers and the individual properties of the constituent materials. In addition, the variation of lay-up configurations of composite laminates allows the designer greater flexibility but complexity in analysis of composite structures. Likewise, the damage and failure in laminated composites are very complicated compared to that of conventional materials. Due to these aspects, modeling of composite laminates is investigated as macromechanical and micromechanical modeling in terms of finite element modeling.

4.1.1. Micromodeling

This approach assumes that the complex microstructure of the composite can be replaced by a representative volume element or unit cell. The representative volume element has a regularly separated arrays of parallel fibers embedded in a homogeneous matrix material so that it can be isolated from the whole composite. The representative volume element has the same fiber volume fraction as the composite laminate and the respective properties of the fiber and matrix individually. The individual constituents are used in the representative volume element model in order to predict the overall response of the composite. This approach provides more physical information at the fiber and matrix level. This is important for the understanding of damage mechanisms and predicting damage progression inside the composite laminates. Moreover, the micromechanical approach can predict the effective properties of composite material

form the knowledge of the individual constituents. This allows the designers to computationally combine different material properties to determine a particular combination that best meets the specific needs.

4.1.2. Macromodeling

The macromechanical approach is concerned with the contributions of each ply to the overall properties, therefore the properties of the fiber and matrix are averaged to produce a set of homogenous, orthotropic properties. In the case of composite laminate there is an additional level of complication which arises as a result of stacking several layers of composites with different orientation and properties. For a given stacking sequence, the stress-strain relations of a composite laminate can be derived and the various coupling mechanisms between in-plane and out of plane deformation modes can be explored. In macromechanical modeling, prediction of failure of a unidirectional fiber reinforced composite is usually accomplished by comparing some functions of the overall stresses or strains to material strength limits. Several failure criteria such as maximum stress, maximum strain, Tsai-Hill, Tsai-Wu have been suggested to predict the failure. These criteria are based on the average composite stress strain states. Macromechanical modeling does not consider the distinctive behavior of the fiber and matrix materials. Although the macromechanical approach has the advantage of simplicity, it is not possible to identify the stress-strain states in the fiber, matrix and their interface. In contrast, in the micromechanical approach, the constituents and their interface can be definitely considered to predict the overall response of the composite as well as the damage initiation and propagation in the composite. (Chen 2000)

4.1.3. Classical Lamination Theory

Classical laminate theory is a widely accepted macromechanical approach for the determination of the mechanical behavior of composite laminates. A laminate is two or more laminae bonded together to act as an integral structural element. A typical laminate is shown in Figure 4.2.

Laminated composite materials are generally orthotropic and typically have exceptional properties in the direction of the reinforcing fibers, but poor properties

perpendicular (transverse) to the fibers. The problem is how to obtain maximum advantage from the exceptional fiber directional properties while minimizing the effects of the low transverse properties. The plies or lamina directions are oriented in several ways such that the effective properties of the laminate match the design requirements. For purposes of structural analysis, the stiffness of such a composite material configuration is obtained from the properties of the constituent laminae. The procedures enable the analysis of laminates that have individual laminae orientations at arbitrary angles to the chosen or natural axes of the laminate. As a consequence overall behavior of a multidirectional laminate is a function of the properties and stacking sequence of the individual layers (Okutan 2001). This is called as the classical lamination theory and predicts the behavior of the laminate if the individual layers are linear-elastic. For laminates where individual plies exhibit inelastic response, additional inelastic strains terms are required (Chen 2000).

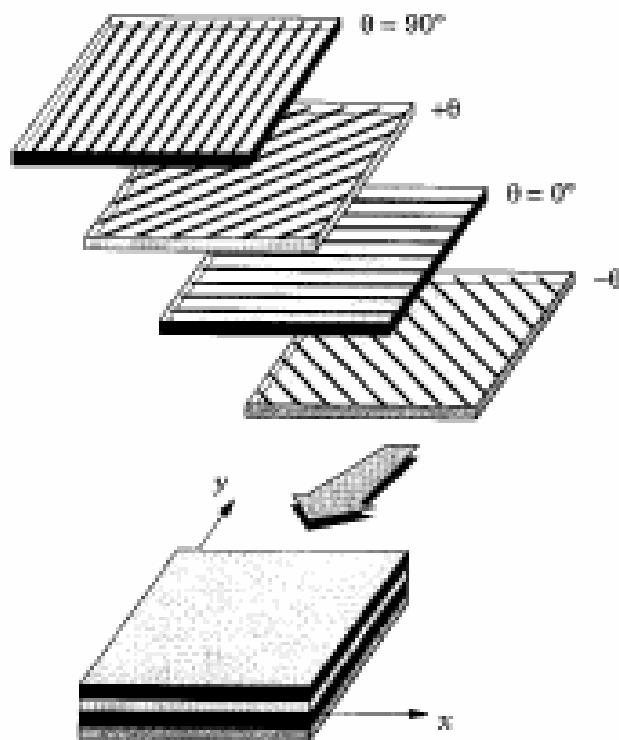


Figure 4.2. A laminate with different fiber orientations
(Source: Okutan 2001)

Knowledge of the variation of stress and strain through the laminate thickness is essential in order to define bending stiffness of a laminate. In the classical lamination

theory, the laminate is assumed as perfectly bonded lamina in load applications (Chou 1991). Moreover, the bonds are assumed to be infinitesimally thin as well as non-shear deformable. Therefore, the displacements are continuous across lamina boundaries so that no lamina can slip. Thus, the laminate acts as a whole. The resultant forces and moments acting on a laminate are obtained by integration of the stresses in each layer or lamina through the laminate thickness.

4.2. Numerical Modeling of Composite Sandwich Structures

Mechanical behaviors of the composite sandwich structures and its constituents were modeled by using finite element analysis technique. For the finite element analysis of the composite sandwich structure ANSYS 11 was used. Composite materials are difficult to model because of their different orthotropic properties, therefore proper element types must be selected, layer configuration must be defined, failure criteria must be defined and lastly modeling and post-processing steps must be done carefully. The most important characteristic of the composite materials is its layered configuration as mentioned before. The properties of the layers have to be specified individually or defined constitutive matrices that are related with the generalized forces, moments and strains by using proper element types.

In this study, composite sandwich structures were modeled by using elements SHELL181 for the core material and SHELL91 for the facesheet material as two of the suggestions for the sandwich structures in the ANSYS structural analysis guide.

SHELL181 is a three dimensional four node element with six degrees of freedom at each node as translations in the x, y, and z directions, and rotations about the x, y and z axes. The geometry, node locations and the coordinate system for this element are shown in Figure 4.3. SHELL181 is well-suited for linear, large rotation and large strain applications. It is also used for layered applications for modeling laminated composite shells or sandwich constructions. The accuracy in modeling composites is governed by the first order shear deformation theory (usually referred to as Mindlin-Reissner shell theory).

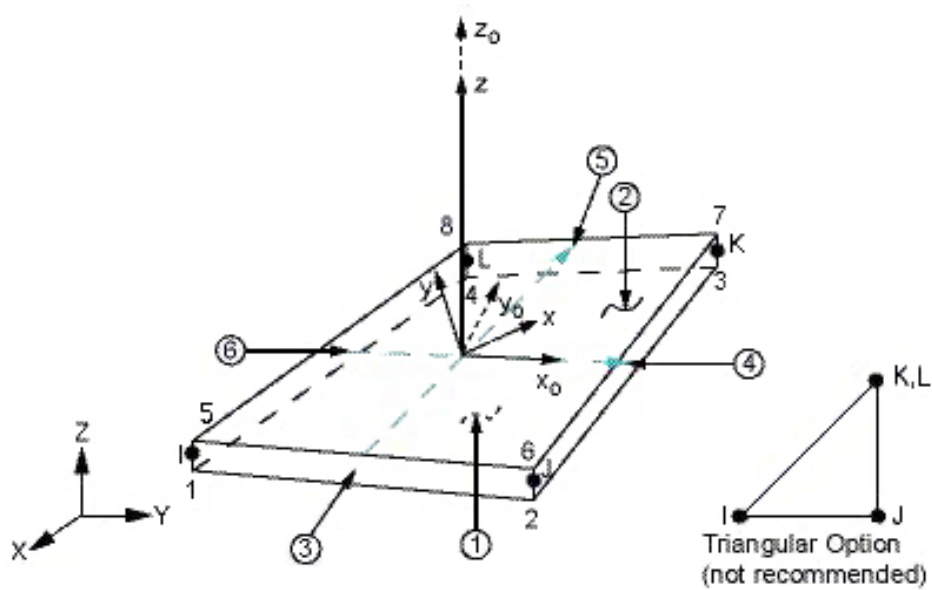


Figure 4.3. Element SHELL181 geometry
(Source: ANSYS Inc. 2007)

SHELL181 can be associated with linear elastic, elastoplastic, creep or hyperelastic material properties. Isotropic, anisotropic, and orthotropic linear elastic properties can be input for elasticity. Stresses, total strains, plastic strains, elastic strains, creep strains, and thermal strains in the element coordinate system are available for output (at all five points through thickness). A maximum of 250 layers is supported and if layers are in use, the results are given in the layer coordinate system.

SHELL91 is a nonlinear structural shell element which can be used for layered applications like sandwich structures. SHELL91 is an eight node element with six degrees of freedom at each node as translations in the nodal x, y and z directions and rotations about the nodal x, y and z axes. The geometry, node locations and the coordinate system for this element are shown in Figure 4.4.

The element is defined by layer thicknesses, layer material direction angles, orthotropic material properties and allows up to 100 layers. The layer configuration is defined from bottom to top in the positive z direction of the element coordinate system (Figure 4.4).

Failure criteria are also defined for the structures in order to find out whether a layer is failed due to the applied loads. There are three widely known failure criteria predefined in the software, they are:

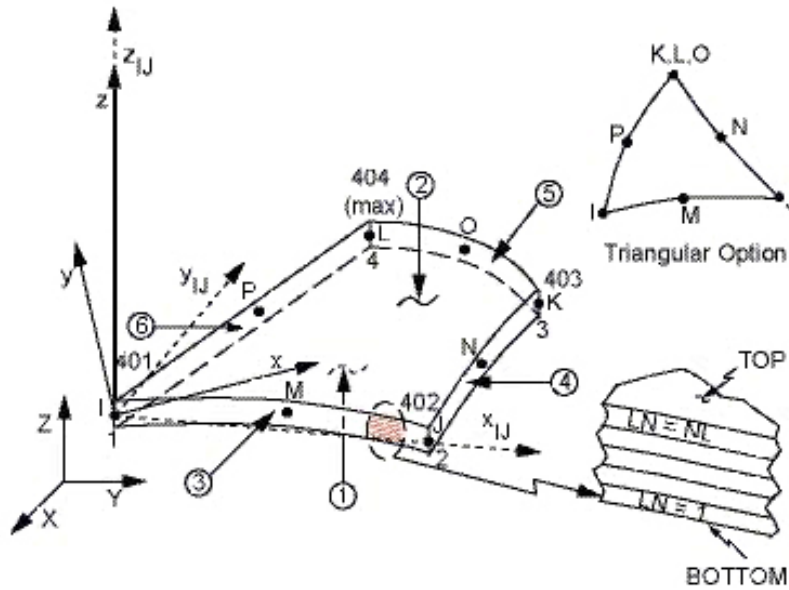


Figure 4.4. Element SHELL 91 geometry
(Source: ANSYS Inc. 2007)

- Maximum Strain Failure Criterion
- Maximum Stress Failure Criterion
- Tsai-Wu Failure Criterion

Failure criteria are orthotropic, therefore it must be taken into account that failure stress and strain values must be given as an input for the program. In this study maximum strain failure criterion is being applied to the structures.

Lastly, modeling and post-processing step is very important in order to verify the input data because for composite materials a large amount of input data is needed (ANSYS Inc. 2007).

4.2.1. Modeling of Facesheets

For the modeling of the composite facesheets, regular rectangular meshes were employed because of the facesheet geometry and SHELL91 element type was used. Test specimens were 25 mm in width, 220 mm in length and 3 mm in depth. The model contains approximately 1000 nodes and the layers were indicated with fiber and epoxy properties individually and the material orientations were also defined in the code. Figure 4.5 shows the view of the test specimen.

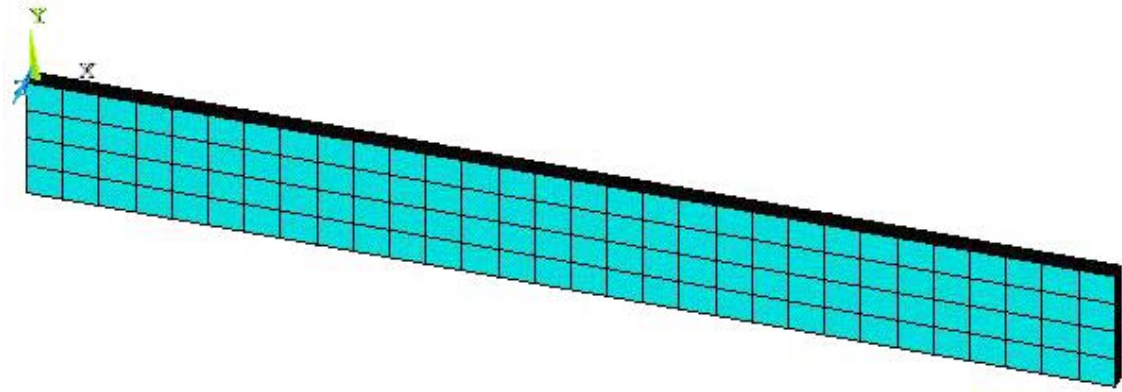


Figure 4.5. Model of the facesheet tensile test specimen

4.2.2. Modeling of Honeycomb Core

For the modeling of the honeycomb core material, SHELL181 element type was used to form regular rectangular meshes for each cell wall of the honeycomb structure. Flatwise compression test specimen was determined as 52 x 52 mm dimensions for each core thickness values. One cell wall of the honeycomb core was first constructed by four elements (Figure 4.6.a) but in order to see the effect of the mesh size, finer meshes were employed and optimum mesh size for one cell wall of the honeycomb core was evaluated. In the optimization process, the same load was applied to each model and the deformation values were collected and their convergence was considered. According to this optimization, cell walls constructed from nine elements is accepted to be optimum (Figure 4.6). In this study, honeycomb core structures were modeled according to this optimization.

For 5 mm core thickness, finite element model had approximately 3527 nodes and 3228 elements. However, for different core thicknesses, the element and node numbers differ according to the thickness of the structure.

4.2.3. Modeling of Sandwich Structures

Composite sandwich structures were modeled by using SHELL91 at facesheets and SHELL181 at honeycomb core material. First, honeycomb core material was modeled according to the optimization, after that the facesheets were modeled on up and down sides of the core in order to generate a sandwich structure. Finite element

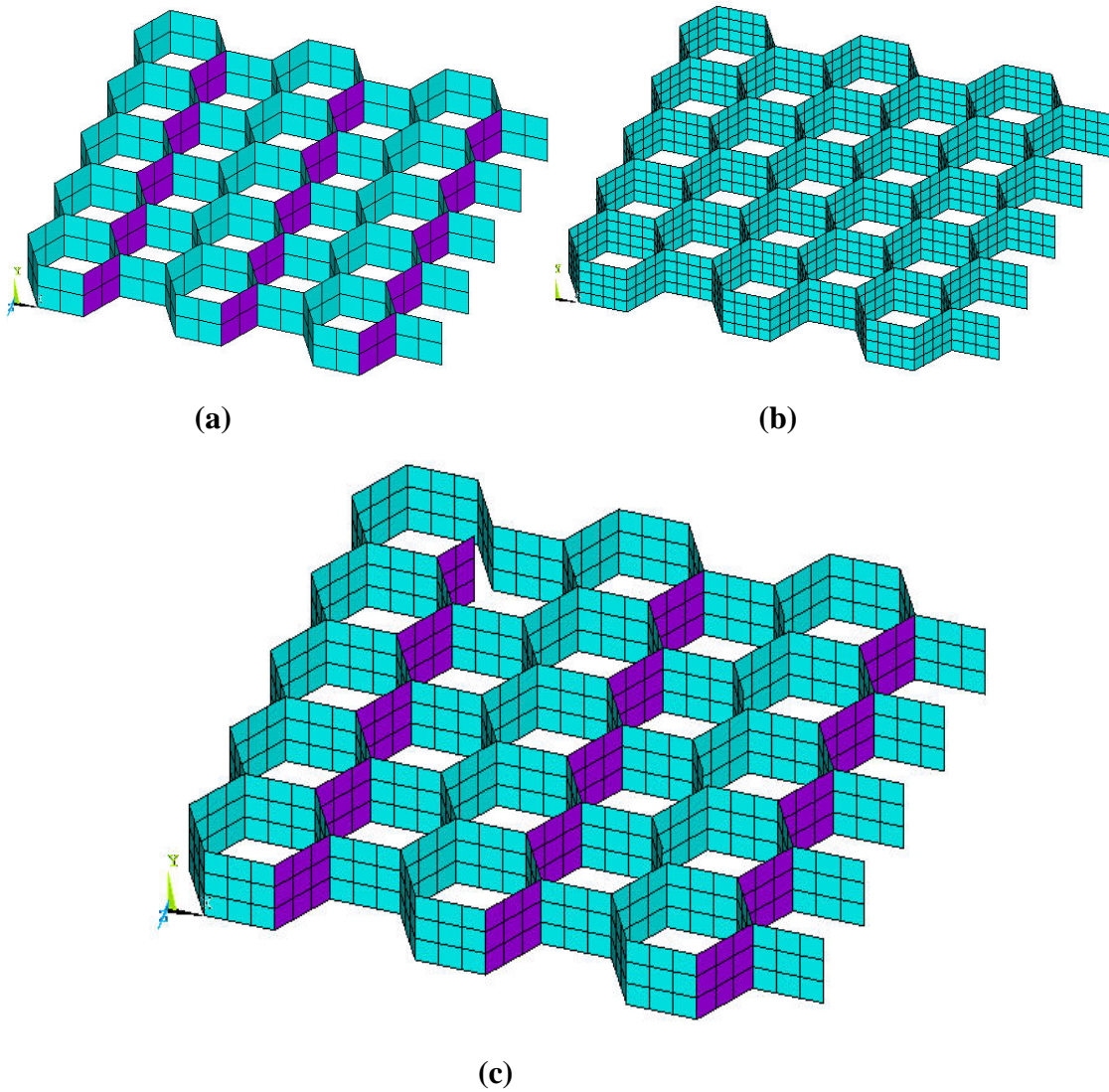


Figure 4.6. Honeycomb core cell wall optimization study models with (a) four elements (b) sixteen elements and (c) nine elements for each cell wall

models were generated for the three point bending, edgewise compression and flatwise compression tests with the specimen dimensions indicated in the related standards. The node and element numbers differ for each test because of the different specimen dimensions.

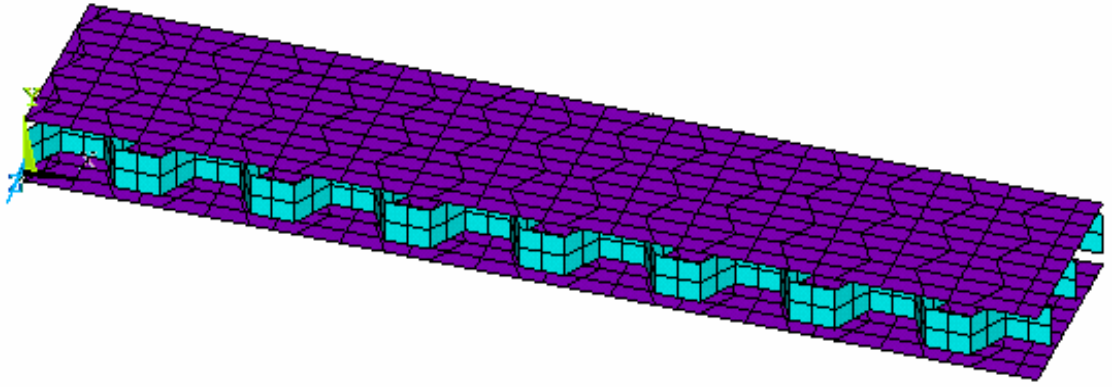


Figure 4.7. Three point bending test specimen with 5 mm core thickness

CHAPTER 5

RESULTS AND DISCUSSION

In this chapter, properties of honeycomb core material, facesheet material and composite sandwich structure are presented. In addition, comparisons of numerical and experimental results on the mechanical properties are given.

5.1. Properties of Honeycomb Core

5.1.1. Flatwise Compression Properties

Figure 5.1 exhibits typical force-stroke graphs of PP based honeycomb core material for various thicknesses loaded under flatwise compression. For each core thickness, mechanical behavior of the material was similar. At the initial stage of the compression loading, it was observed that cell walls deformed linearly. Core cell walls buckled due to the local buckling, which limited the ultimate strength, and a relatively sudden collapse took place after the maximum load levels. From these curves it was also been observed that the thicker core materials experience the maximum force levels at lower deformation values than those for the thinner ones. This is due to the buckling of the longer cell walls at lower stroke values.

Figure 5.2 shows the flatwise compressive strength and modulus values for the PP core material as a function of the core thickness. As seen from the figure that both compressive strength and modulus values of the honeycomb PP core increases as the core thickness increases.

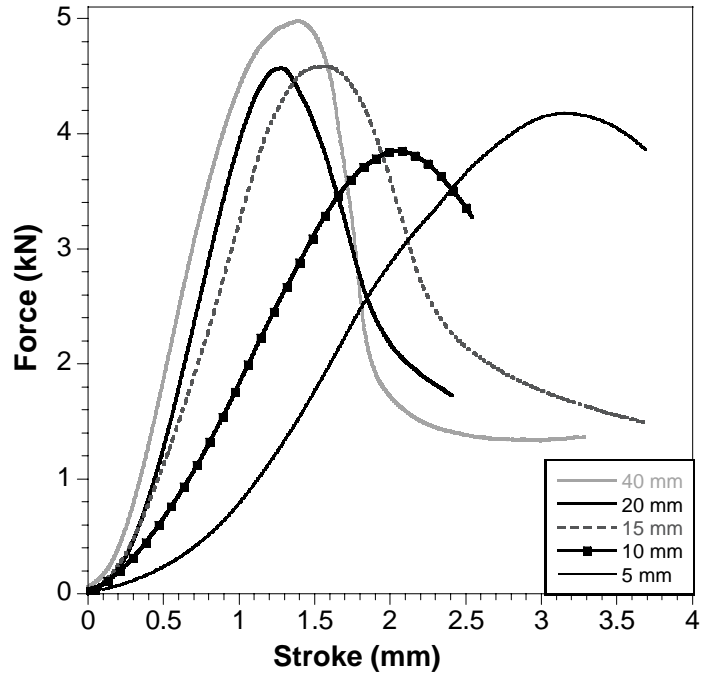


Figure 5.1. Flatwise compressive behavior of PP based honeycomb core material for each thickness

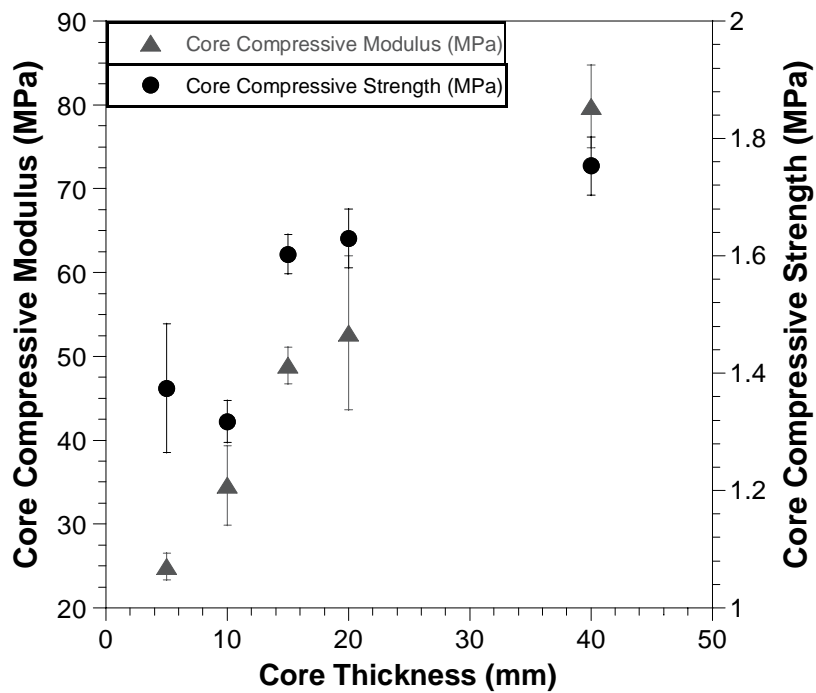


Figure 5.2. Core compressive modulus and strength values with respect to core thickness

5.1.2. Cell Wall Thickness

The increase of the core compressive modulus with the core thickness increment was related with the cell wall thickness increment with respect to the core thickness. For that reason, cell wall thicknesses were measured for each of the core material. In Figure 5.3 the variation of the normalized cell wall thickness in accordance with the normalized core thickness increment is shown.

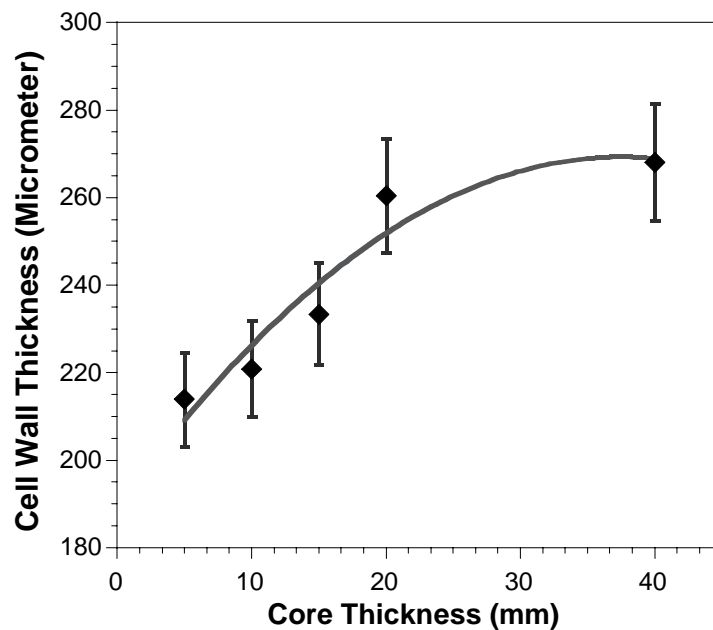


Figure 5.3. Cell wall thickness variation with respect to core thickness

5.2. Properties of Facesheet Material

5.2.1. Fiber Volume Fraction

Fiber volume fraction of the produced E-glass fiber/epoxy composite facesheets was measured by matrix burn-out test. The average fiber volume fraction was measured as 0.38 ± 0.0076 for the composite facesheets.

5.2.2. Tensile Properties

Figure 5.4 shows tensile stress-strain response of E-glass fiber/epoxy composite facesheets. Stress-strain response of the facesheet is non-linear and there is a sudden drop after the maximum stress at which failure occurs. The average tensile strength and modulus values of the E-glass fiber/epoxy facesheet were found to be 270 ± 18.9 MPa and 14.5 ± 0.58 GPa, respectively.

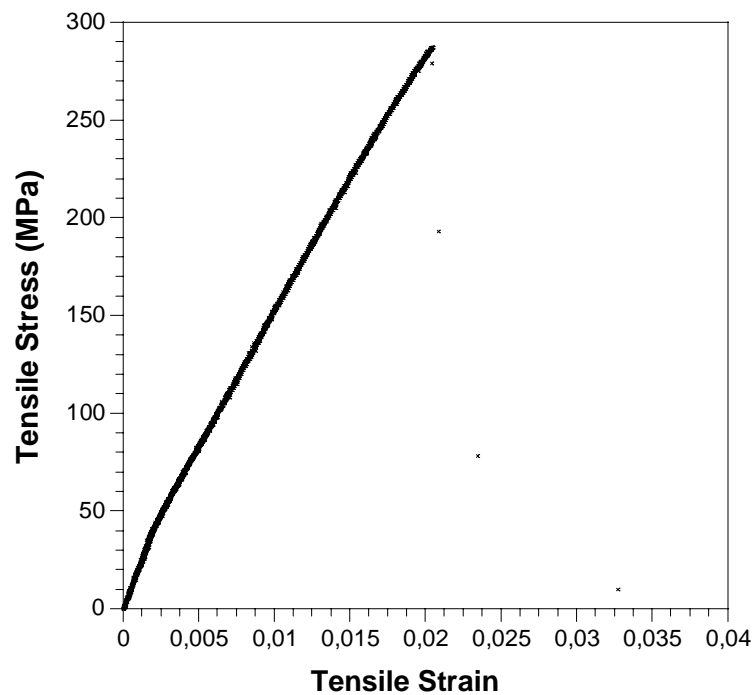


Figure 5.4. Typical tensile stress-strain response of E-glass fiber/epoxy composite facesheets

5.2.3. Compressive Properties

The compressive stress strain response of the composite facesheets loaded along the ply-lay up and in-plane directions are given in Figure 5.5. On the behalf of the results obtained, the compressive strength values of the composite facesheets were found to be 438 ± 31 MPa and 314 ± 29 MPa for ply-lay up and in-plane directions, respectively. The ply-lay up compressive modulus of the facesheets was measured to be 4.1 ± 0.8 GPa, which is about 75% lower as compared to their in-plane compressive

modulus (7.3 ± 1.1 GPa). In particular, compressive strength and modulus values of the composite facesheets are higher in ply-lay up direction than in-plane direction.

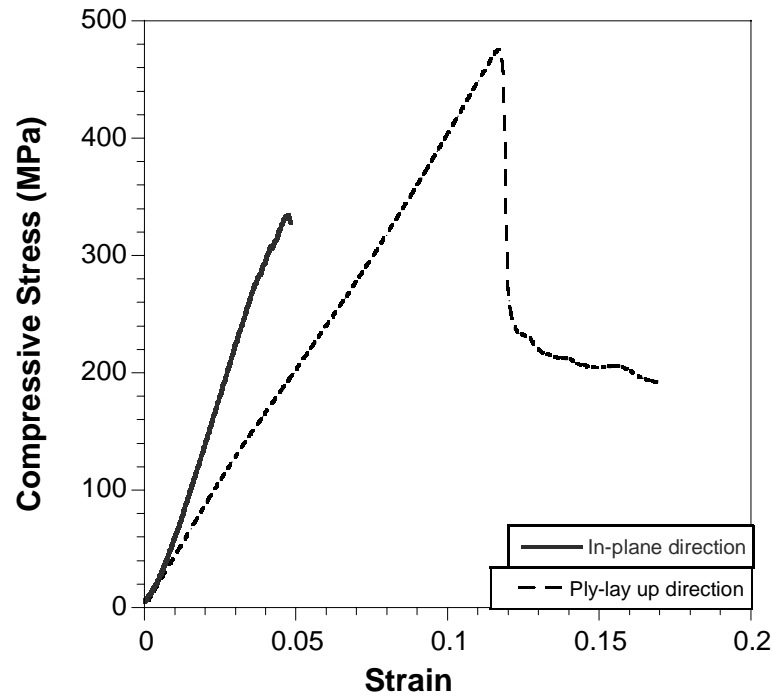


Figure 5.5. Stress strain behavior of the compressive properties of facesheet material along ply-lay up and in-plane directions

Figure 5.6 depicts the photo of a test specimen failed under ply-lay up compressive loading. As seen in the figure, failure occurred within the corresponding specimen, making 45° angle to the loading direction in the way as expected.

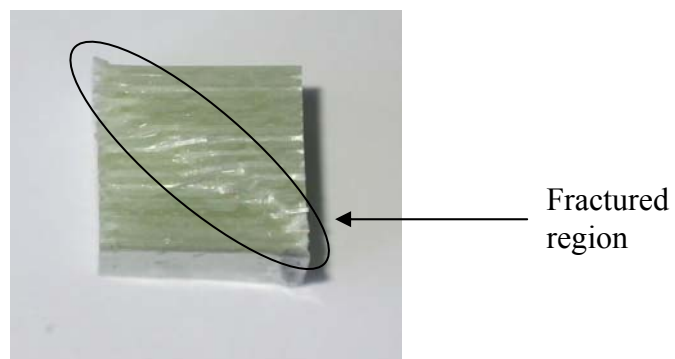


Figure 5.6. Failure direction of the ply-lay up specimen loaded in compression test

5.2.4. Flexural Properties

Flexural stress-strain response of the composite facesheet is given in Figure 5.7. Stress values increases linearly in the elastic region. Maximum stress occurs at the mid span in three point bending configuration. Above the maximum stress, the composite layers delaminate and failure occurs. The average flexural strength and modulus values of the facesheet material were found to be 490 ± 44.1 MPa and 14 ± 0.28 GPa, respectively.

The loading in the bending test consists of tension, compression and shear forces. The laminates tested along the fiber direction and they generally experienced brittle failure in the outer ply as delamination on the tensile surface. The delamination starts at the middle of the specimen because of the maximum bending moment, in the middle section of the tensile surface fiber rupture occurred. Delamination was observed on both tensile and compressive surfaces of the specimens. Until the fiber failure, large deflection was achieved. In the literature, the similar test results were obtained (Wang 2002).

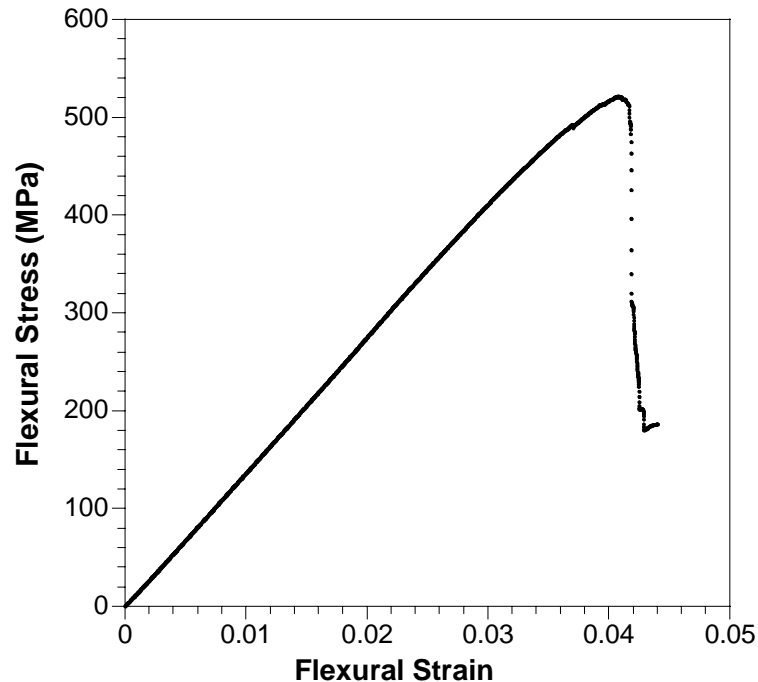


Figure 5.7. Typical stress vs. strain curve for the composite facesheets under flexural loading

5.2.5. Interlaminar Shear Properties

Short beam shear test was applied to the facesheet material in order to find out the interlaminar shear strength. According to the test results, average interlaminar shear strength of the facesheets was found to be 29 ± 0.87 MPa. It was observed that typical failure mode, in the short beam test was the delamination of the plies.

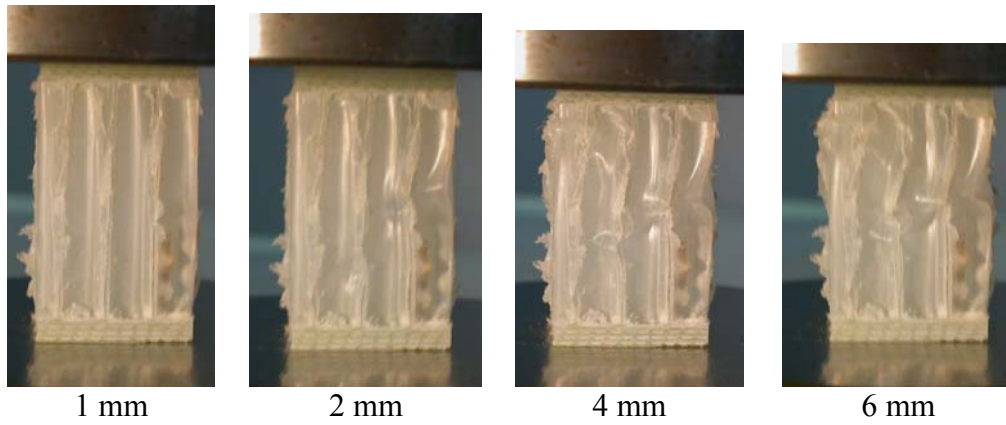
5.3. Properties of Composite Sandwich Structures

5.3.1. Flatwise Compressive Properties

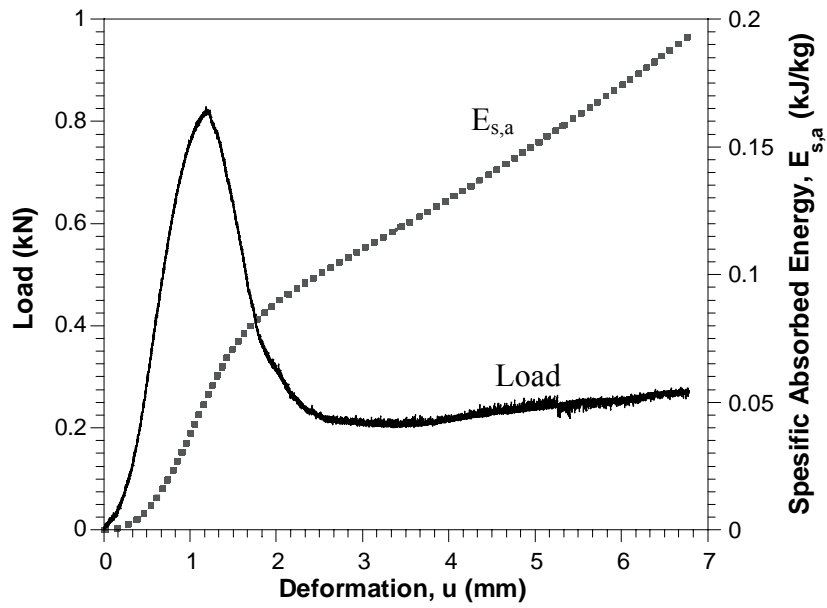
The collapse sequence images and load-deformation behavior of the composite sandwich structures under flatwise loading are presented in Figure 5.8.

It was observed that up to the maximum load level a linear load-deformation relation took place. After the maximum load level, system collapsed and a large drop in the load level occurred. It was observed that the cause of the drop is the bending and local buckling of the cell walls. The load continued to increase with a small slope after the initial drop. This increase in load capacity at this region is caused by the densification of the folded cell walls. In Figure 5.8.b, specific absorbed energy (absorbed energy/weight of the composite, $E_{s,a}$) is also illustrated. At the point of collapse, energy absorption rate decreased as the slope of the $E_{s,a}$ curve decreased. The deformation of the structure under compressive load is illustrated by the images given in Figure 5.8.a. As seen in the first picture, at the initial region no bending at the cell walls was observed. After the maximum load level bending of the cell walls occurred.

Figure 5.9 shows the flatwise compression modulus and strength values as a function of core thickness. As seen from the figure, the compression modulus values increase with increasing core thickness. This behavior is similar to the behavior observed in flatwise compression tests of the constituent core material (Figure 5.2). This is an expected result that the FWC properties of sandwich structures are dependent on the core material behavior (Borsellino, et al. 2004). Therefore, the increase of the modulus of the composite sandwich with the increase of cell wall thickness (a), is similar to those given in Figure 5.2 for PP core itself.



(a)



(b)

Figure 5.8. Behaviour of composite sandwich structures under flatwise loading: (a) collapse sequence images, (b) load-deformation graph of the test specimen and the specific absorbed energy, $E_{s,a}$ graph during the test

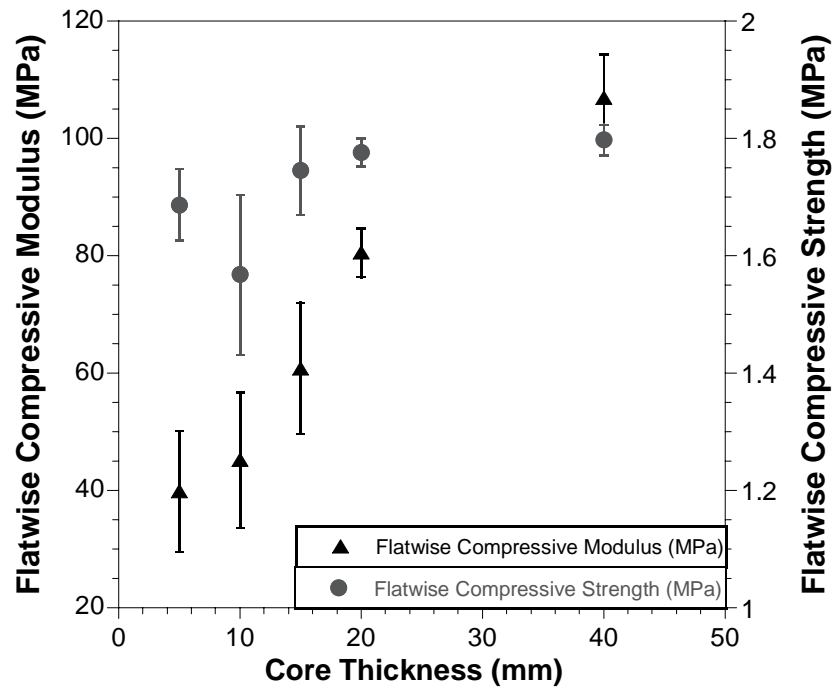


Figure 5.9. Flatwise compressive strength and modulus values of composite sandwich structures as a function of core thickness

In Figure 5.10 failure mechanisms of the sandwich structures are given. From the images it can be observed that when the core thickness increased, more folding was observed in the honeycomb cell walls for the same deformation values. Therefore, the absorbed energy by the sandwich structures increase as the core thickness increases (Figure 5.11).

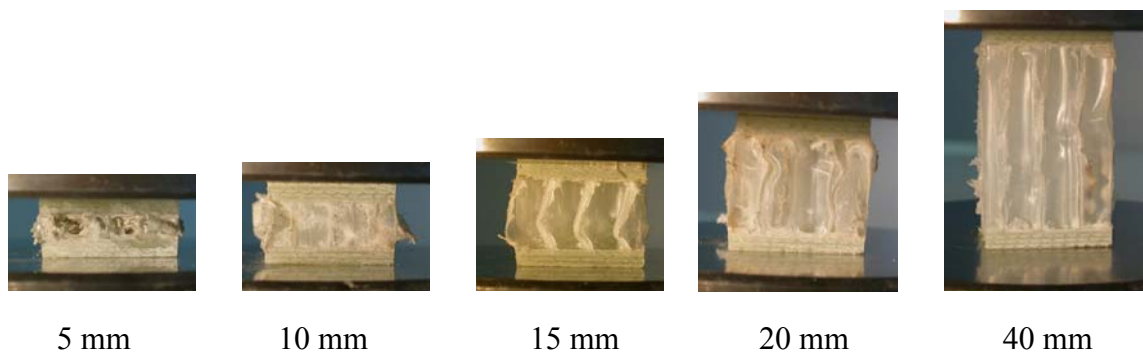


Figure 5.10. Failure mechanisms for sandwich structures with various core thicknesses under flatwise compression loading (The stroke is 3 mm for each core)

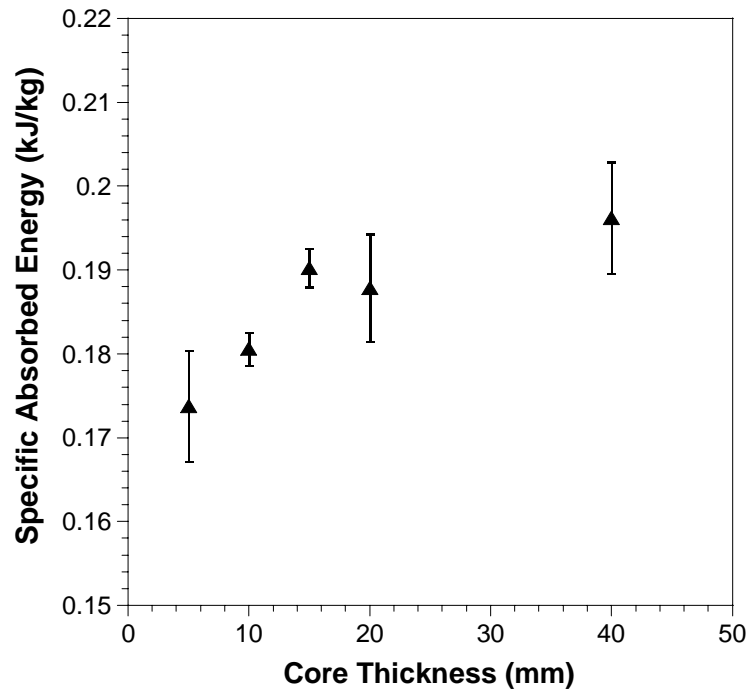
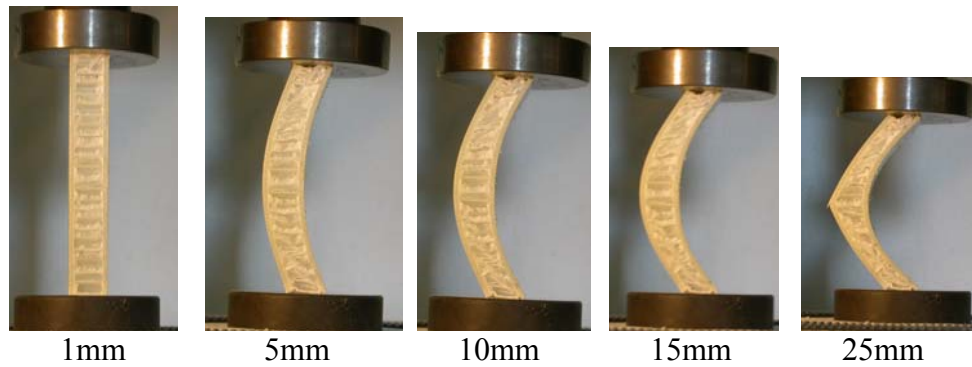


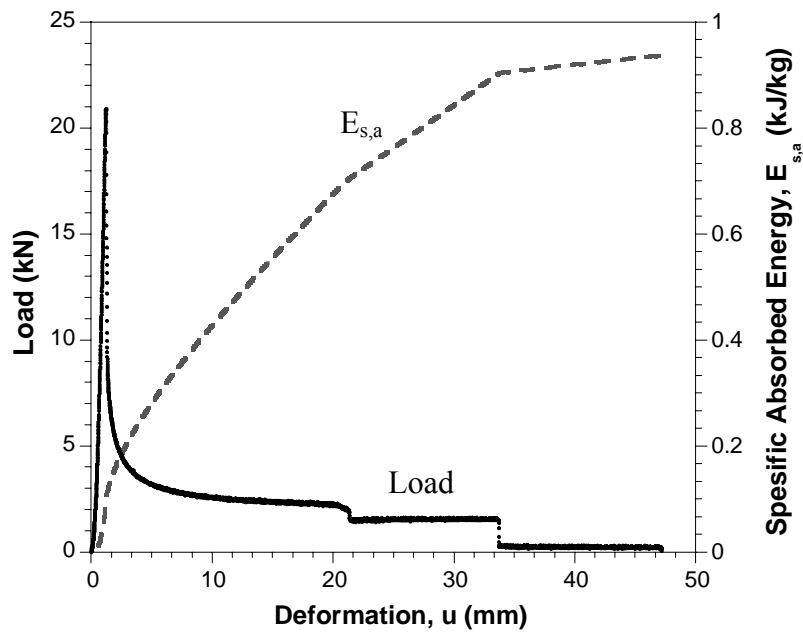
Figure 5.11. Specific absorbed energy values of the composite sandwich structures with respect to core thickness increment

5.3.2. Edgewise Compressive Properties

In Figure 5.12 collapse sequence images and typical load-deformation graph of a typical sandwich structure are given. In the load-deformation graph, area under the curve was calculated and divided by the weight of the specimen; therefore specific absorbed energy was obtained. The load-deformation curve (Figure 5.12.b) has a linear portion at the beginning. Afterwards, facesheet buckling within the sandwich panel initiated with the de-bonding of the core and facesheets at the edge of the panels in contact with the crossheads. Failure occurred due to shear at the interface between the core and the facesheet laminate; on the compression side of the core. On the opposite side that is under tension, the core remained perfectly bonded to the facesheet. The deflection of the panel increased as the load was applied. At large deformation ratios, facesheets fractured. The fracture of the facesheets started from the tensioned face and continued through the thickness (Figure 5.12.a). This mode of collapse is called “sandwich panel column buckling” as also reported in the literature (Borsellino, et al. 2004). In this stage, bending resistance of the sandwich structure decreases, which also cause the decrease of energy absorption.



(a)



(b)

Figure 5.12. Behaviour of the composite sandwich structures under edgewise loading: (a) collapse sequence images of the specimen and (b) load-deformation graph of the test specimen and the specific absorbed energy, $E_{s,a}$ during the test

In the edgewise compression test, facesheets are the main load carrying members. The core materials increase the strength of the system through coupling the facesheets to each other and increasing the buckling capacity. In Figure 5.13 it can be observed that a sudden increase occurred at specific core thickness values.

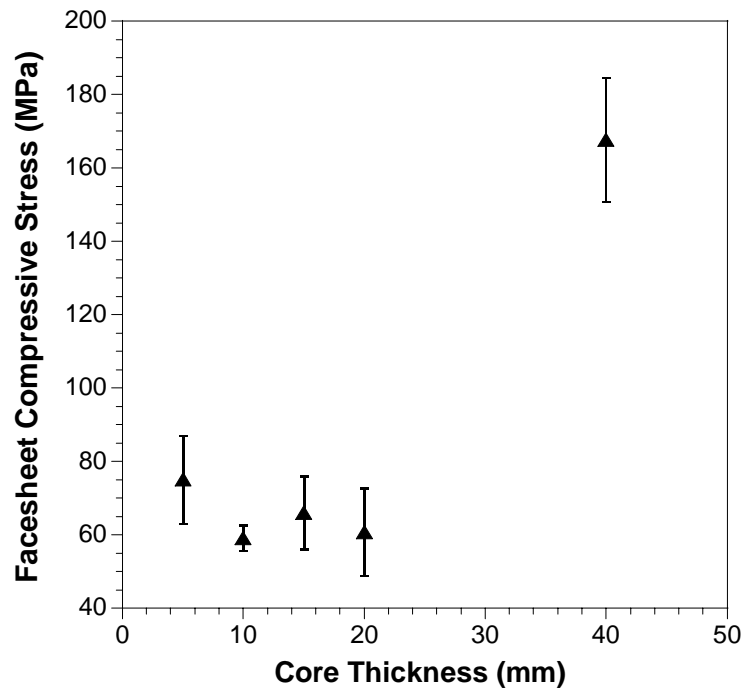


Figure 5.13. Facesheet compressive stress as a function of core thickness increment

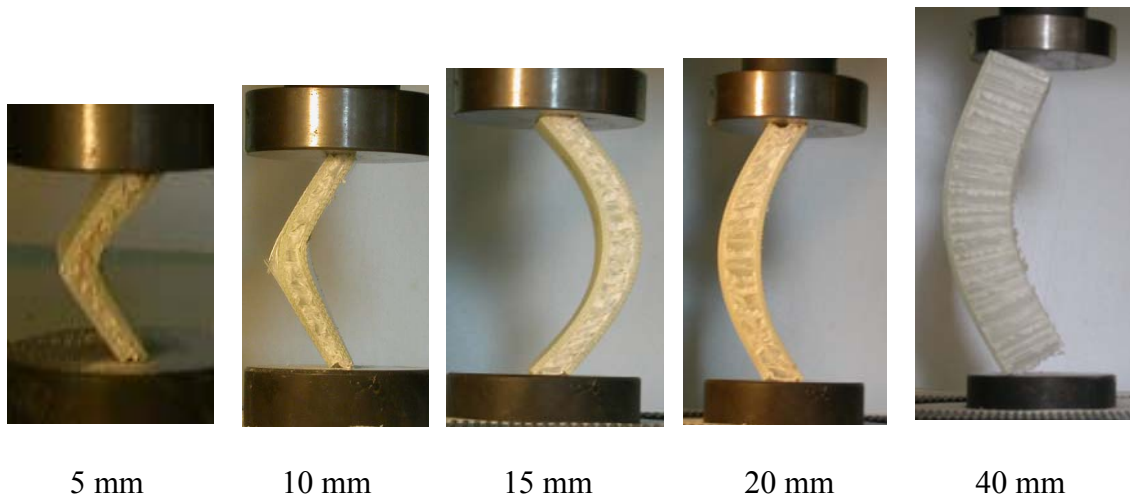


Figure 5.14. Failure mechanisms for sandwich structures with all different core thicknesses under edgewise compression loading

As the core thickness increased, failure mechanisms of the sandwich structures changed as well. Sandwich structures with thin core materials failed under bending while delamination occurred within the composites with thicker core materials (Figure 5.14). As reported in the literature, energy absorption of the sandwich structures

changes with the failure mechanism and in Figure 5.15 the variation of the energy absorption with respect to the core thickness can be seen.

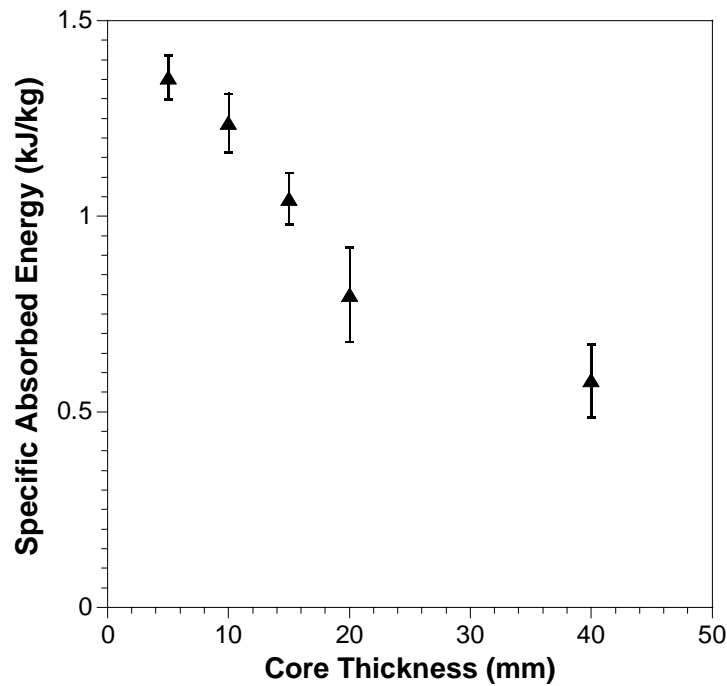


Figure 5.15. Energy absorption values of the composite sandwich structures with core thickness increment

5.3.3. Flexural Properties

Three point bending test was applied to the sandwich structures in order to evaluate the core shear stress and facesheet bending stress variation in accordance with the core thickness increase. It can be seen from Figure 5.16 that core shear stresses at the peak load and sandwich beam deflection decrease as the core thickness increases.

On the other hand, it can be observed from Figure 5.17 that panel bending stiffness at the initial linear portion and panel rigidity increases with increasing core thickness.

Sandwich structure facesheet bending stress as a function of the core thickness is given in Figure 5.18.

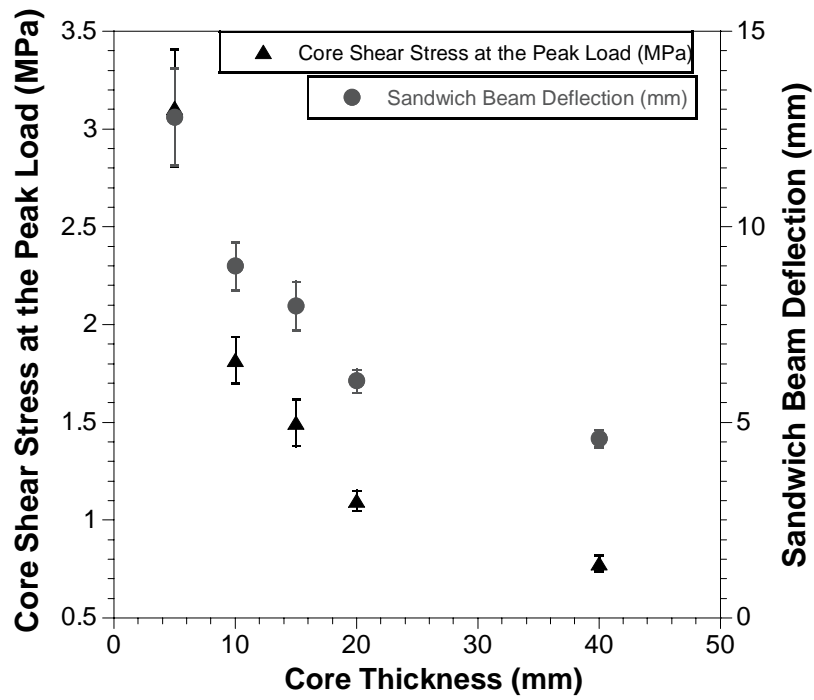


Figure 5.16. Core shear stress and sandwich beam deflection tendency with increasing core thickness

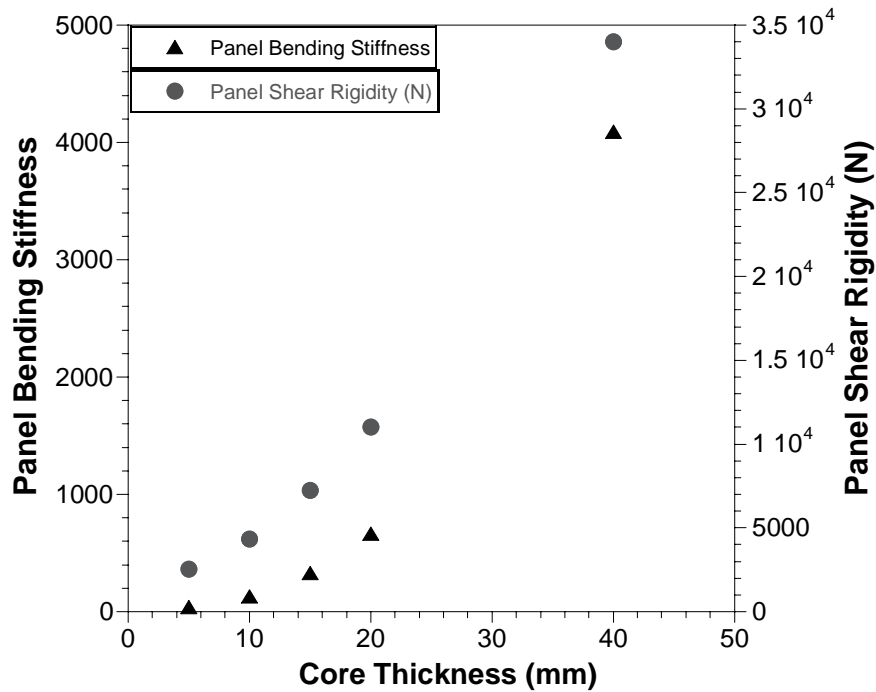


Figure 5.17. Panel bending stiffness and panel shear rigidity tendency of the composite sandwich structures with core thickness increase under flexural loading

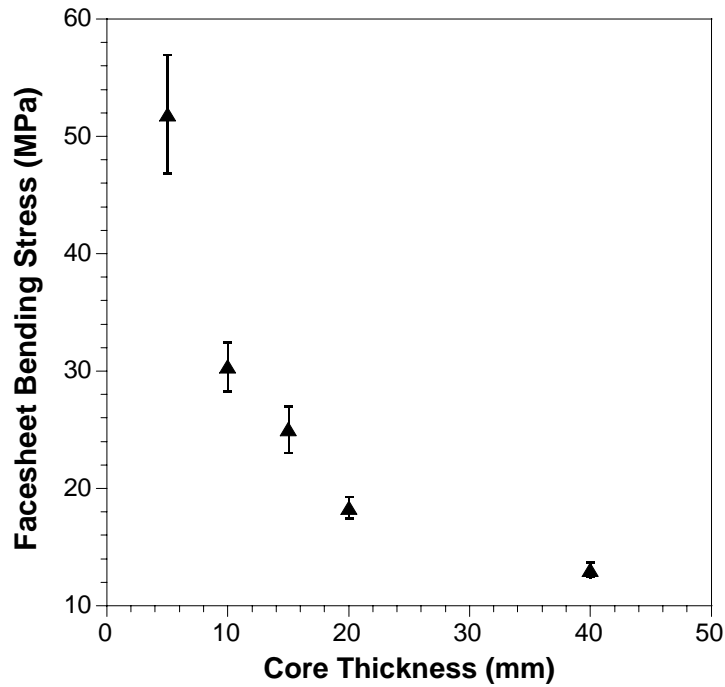


Figure 5.18. Facesheet bending stress of the composite sandwich structures with core thickness increment

5.3.4. Interlaminar Fracture Toughness

Core material/facesheet plate interface fracture toughness values were evaluated by Mode-I fracture toughness test. In Figure 5.19, Mode-I fracture toughness values of the composites for various core thickness are given as a function of delamination length increase. The average crack initiation values were found to be 80 J/m^2 for each core thickness and the crack propagation values were measured as 800, 600, 1000, 500, 900 J/m^2 for 5, 10, 15, 20, 40 mm core thicknesses, respectively. It was observed that there is not a significant relation between core thickness increase and fracture toughness values, as expected. Fracture toughness value is not related with the honeycomb core and cell wall thickness increments. The fracture mode was observed to be a continuous crack growth.

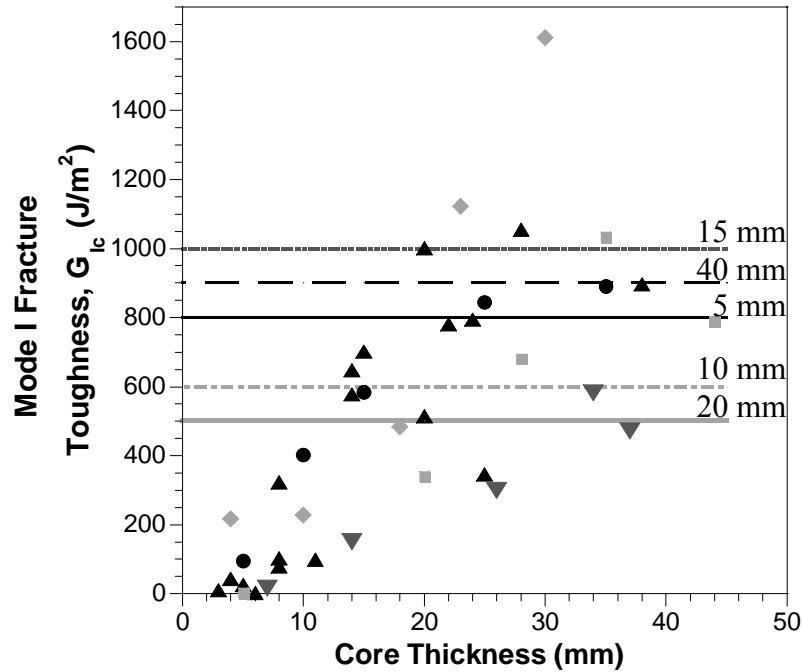


Figure 5.19. Interlaminar fracture toughness values of the composite sandwich structures with respect to the core thickness increment

5.4. Comparison of Numerical and Experimental Results

As a part of this study, mechanical behaviors of the composite sandwich structures and their constituents were numerically modeled. PP based honeycomb core was modeled for the flatwise compression test, E-glass fiber/epoxy facesheet was modeled for tension test and composite sandwich structure was modeled for flatwise compression, three point bending and edgewise compression tests. Experimental and finite element modeling results were compared.

5.4.1. Facesheet Material

Tensile test boundary conditions were defined in the code as clamped at one width. On the opposite width the deformation was applied in the x direction and the nodes were fixed in y and z directions. The deformed shape of the facesheet is shown in Figure 5.20. The dashed line represents the specimen shape before deformation.

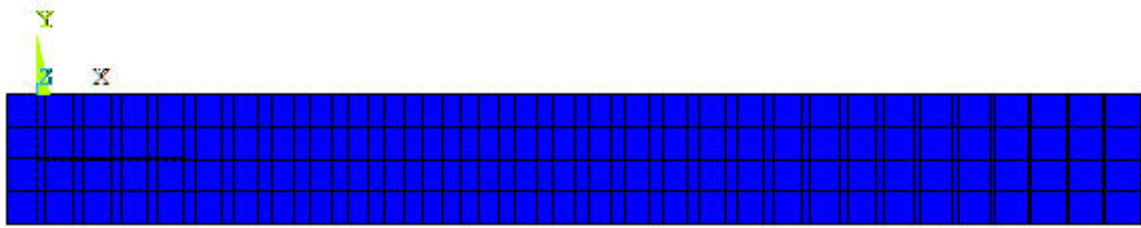


Figure 5.20. Deformed and undeformed shape of the facesheet tensile test specimen

The tensile behavior of the composite facesheet is shown in Figure 5.21. According to this figure, the predicted data and experimental results are similar to each other.

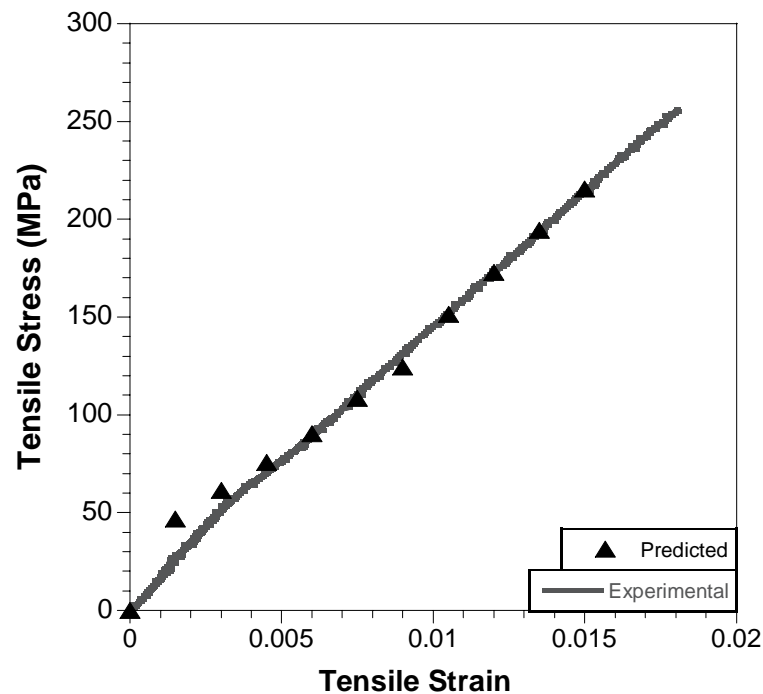


Figure 5.21. Comparison of predicted and experimental data of facesheet tensile test

5.4.2.Honeycomb Core

PP based honeycomb core material was modeled with SHELL181 element and as mentioned before 9 elements were used for each cell wall of the honeycomb shape. Also a flat plate was placed upon the compression specimen in the model because of the long calculation time and capacity of the purchased program. In the flatwise compression test, the specimen was fixed on the bottom surface. Deformation was

applied from several points on the plate and the reaction forces of those points were summed up in order to find the predicted applied load.

Comparison of experimental and predicted data for the honeycomb core compression test is given in Figure 5.22. Experimental test data were shifted in order to see the coherence better.

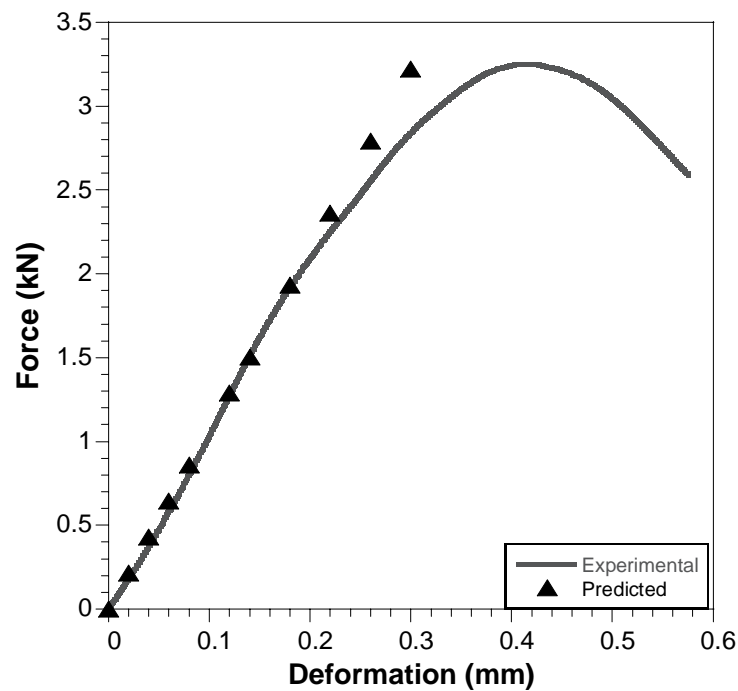


Figure 5.22. Force deformation graph of experimental and predicted flatwise compression test data

As it can be seen from Figure 5.22, there is a good agreement in the elastic region between experimental and predicted data.

5.4.3. Sandwich Structure

Composite sandwich structures were modeled with SHELL91 in facesheets and SHELL181 in honeycomb core structures. Finite element modeling was done for the three point bending test. In this test, the lower facesheet was fixed along the lines apart from each other by the span length and these lines coincided with the supports in the experiment. The deformation was given from the middle line nodes in the y direction.

Comparison of experimental and predicted data for the three point bending test is given in Figure 5.23. In the elastic region the test data and finite element modeling results were fitting each other. In the following regions inelastic behavior was observed in the experiments however in the modeling it was not implemented into the code because of the complexity of the program.

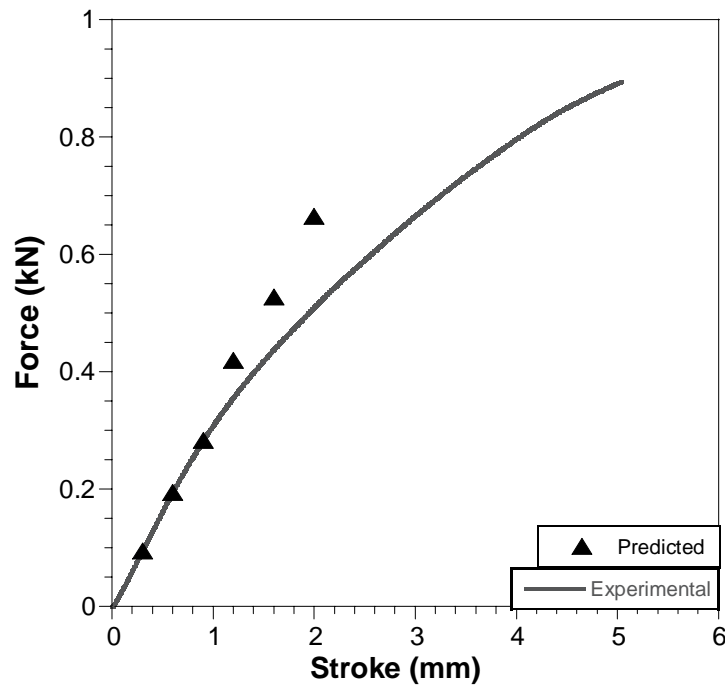


Figure 5.23. Predicted and experimental force deformation comparison graph of the sandwich structure

CHAPTER 6

CONCLUSION

In this study, the mechanical properties of composite sandwich structures fabricated with $0^{\circ}/90^{\circ}$ E-glass fiber/epoxy facesheet and polypropylene (PP) based honeycomb core were evaluated. The individual behavior of the PP based honeycomb core material and E-glass fiber/epoxy facesheets were also determined by performing related ASTM tests on these materials.

Application of the flatwise compression tests to the honeycomb core material showed that core material compressive strength and modulus increased with the core thickness as the honeycomb cell wall thickness increase. In the flatwise compression test, honeycomb core cell walls buckled locally and densified.

Composite facesheet material was also tested and it was observed that the compressive modulus and strength values are higher in ply lay-up direction than in-plane direction. In the flexural test, the delamination started and failure occurred at the midspan and brittle failure was observed.

For the sandwich structures, based on flatwise compression test, it was observed that composite sandwich structures with honeycomb core material deformed similarly with the core material itself. It was also observed that only the core material influences the flatwise compressive properties of sandwich panel. As the core thickness increased failure mechanism changed, a higher fraction of folding was observed with the thicker cores for the same deformation, therefore, energy absorption increased as well. Under the edgewise compression loading of sandwich structures, facesheets buckled and failure occurred at large deformation values, however buckling load was increased because of the coupling of the facesheets. In the edgewise compression test, “sandwich panel column buckling” collapse mode, which is not the most efficient mode for crash energy absorption, was observed. Failure mechanism of the sandwich structures also changed with core thickness increment, thick cored sandwich structures delaminated while thin cored ones failed under bending. Three point bending test results showed that core shear stress, sandwich beam deflection and facesheet bending stress at the peak load decreased while the panel bending stiffness increased with the core thickness

increment. Mode-I interlaminar fracture toughness test showed that there is no significant relation between core thickness increment and fracture toughness values.

The finite element modeling of the composite sandwich structures and its constituents were also investigated in this study. For the modeling of the PP based honeycomb material, three dimensional, 4-noded SHELL181 element was used. For the composite facesheet material, 8-noded nonlinear structural SHELL91 element was used. According to the finite element model, good agreement was observed in the elastic region.

In summary, core thickness increment has been found to be important for the flatwise and edgewise compressive and flexural behaviors of the composite sandwich structures, however, no significant effect was found on the interlaminar fracture toughness values. Finite element modeling was found to be useful for the elastic region and it can be improved for the prediction with the inelastic region.

REFERENCES

- Adams, Donald F. 2006. Sandwich panel test methods. *High Performance Composites*, no. 5: 4-6. <http://www.compositesworld.com/> (accessed January 21, 2007).
- ANSYS Incorporation. 2007. *Structural Analysis Guide*. Canonsburg: ANSYS Incorporation.
- ASM International Metals Park. 1987. *Engineered Materials Handbook Vol. 1. Composites*. Ohio: ASM International Metals Park.
- Borsellino, C., Calabrese, L. and A. Valenza. 2004. Experimental and numerical Evaluation of Sandwich Composite Structures. *Composite Science and Technology*, 64:1709-1715.
- Callister, William D. 2000. *Materials Science and Engineering An Introduction*. India: Wiley.
- Cantwell, W.J., Scudamore, R., Ratcliffe, J. and P. Davies. 1999. Interfacial fracture in sandwich laminates. *Composites Science and Technology*. 59: 2079-2085.
- Chen Y. 2000, Finite Element Micromechanical Modeling of Glass Fibre Epoxy Cross-ply Laminates. *University of Alberta Thesis of MS*.
- Chou, Tsu-Wei. 1991. *Microstructural design of fiber composites*. Cambridge: Cambridge University Press.
- Davalos, J.F. and A. Chen. 2005. Buckling behavior of honeycomb FRP core with partially restrained loaded edges under out-of-plane compression. *Journal of Composite Materials* 39: 1465-1485.
- Davies, G.A.O., Hitchings, D., Besant, T., Clarke, A. and C. Morgan. 2004. Compression after impact strength of composite sandwich panels. *Composite Structures*. 63: 1-9.
- El Mahi, A., Farooq, M. K., Sahraoui, S. and A. Bezazi. 2004. Modelling the flexural behaviour of sandwich composite materials under cyclic fatigue, *Materials and Design* . 25: 199-208.
- Ercan H. 2006. Uçak Sanayiinde Kullanılan Bal Peteği Kompozitlerin Mekanik Davranışlarının İncelenmesi. Yıldız Teknik Üniversitesi Thesis of PhD.

- Felippa, Carlos A. 2004. *Introduction to the Finite Element Method*. University of Colorado, Colorado. <http://www.colorado.edu/> (accessed February 15, 2008).
- Glenn, C.E. and M.W. Hyer. 2005. Bending behavior of low-cost sandwich plates. *Composites: Part A*. 36: 1449–1465.
- Göde, E. 2007. Savaş uçaklarında yapısal malzeme olarak kullanılan sandviç kompozitlerin hasar tespiti ve onarımının incelenmesi. *Eskiehir Osmangazi Üniversitesi Thesis of MS*.
- Guedes, R.M. 2008. *Creep of polymer-matrix based composite laminates*. Porto: Universidade do Porto Faculdade de Engenharia.
- Jianga, H., Huang, Y. and C. Liub. 2004. Fracture analysis of facesheets in sandwich composites. *Composites: Part B*. 35: 551–556.
- Liang, S. and H.L. Chen. 2006. Investigation on the square cell honeycomb structures under axial loading. *Composite Structures*. 72: 446–454.
- Mamalis, A.G., Manolakos, D.E., Ioannidis, M.B. and D.P. Papapostolou. 2005. On the crushing response of composite sandwich panels subjected to edgewise compression: experimental. *Composite Structures*. 71: 246–257.
- Moura, M.F.S.F., Campilho, R.D.S.G., Ramantani, D.A. and A.T. Marques. 2008. *Repair of Composites and Sandwich Structures*. Porto: Universidade do Porto Faculdade de Engenharia.
- Nguyen, M.Q., Jacombs, S.S., Thomson, R.S., Hachenberg, D. and M.L. Scott. 2005. Simulation of impact on sandwich structures. *Composite Structures*. 67: 217-227.
- Norlin, P. and S. Reuterlöf. 2002. The role of sandwich composites in turbine blades. *Reinforced Plastics*. 3: 32-34.
- Okutan, B. 2001. Stress and failure analysis of laminated composite pinned joints. *Dokuz Eylül University Thesis of PhD*.
- Rocca, S.V. and A. Nanni. 2005. *Mechanical characterization of sandwich structure comprised of glass fiber reinforced core: Part I*. Missouri University of Science and Technology. <http://utc.mst.edu/> (accessed June 25, 2007)
- Smith, S.A. and K.N. Shivakumar. 2001. Modified Mode-I Cracked Sandwich Beam (CSB) Fracture Test. *American Institute of Aeronautics and Astronautics*. 1221-1232.

Turgut T. 2007, Manufacturing and Structural Analysis of a Lightweight Sandwich Composite UAV Wing. *Middle East Technical University Thesis of MS.*

Vinson, Jack R. 1999. *The Behavior of Sandwich Structures of Isotropic and Composite Materials.* USA: Technomic Publishing.

Zureick, A., Shih, B. and E. Munley. 1995. Fiber Reinforced Polymer Bridge Decks. *Structural Engineering Review.* 7: 257-266.